atmosphere

MDPI

Article

Mapping Heatwave Socioeconomic Exposure in the Chinese Mainland for the Period of 2000–2019

Wei Wu [1,2], Qingsheng Liu [1,2,3,*], He Li [1], Chong Huang [1] and Weiming Cheng [1]

[1] State Key Laboratory of Resources and Environmental System, Institute of Geographic Sciences and Natural Resources Research, Chinese Academy of Sciences, Beijing 100101, China; wuwei@lreis.ac.cn (W.W.); lih@lreis.ac.cn (H.L.); huangch@lreis.ac.cn (C.H.); chengwm@lreis.ac.cn (W.C.)
[2] University of Chinese Academy of Sciences, Beijing 100049, China
[3] Jiangsu Center for Collaborative Innovation in Geographical Information Resource Development and Application, Nanjing 210023, China
* Correspondence: liuqs@lreis.ac.cn

Abstract: Mounting evidence suggests an increasing heatwave risk in the Chinese mainland, posing notable threats to public health and the socioeconomic landscape. In a comprehensive analysis, considering both climate and socioeconomic factors, including Gross Domestic Product (GDP) and population dynamics, we systematically evaluated the spatiotemporal distribution of heatwave socioeconomic exposure in the Chinese mainland from 2000 to 2019, utilizing a more comprehensive heatwave hazard index (HHI) that synthesizes heatwave intensity, frequency, and duration as climate factor for the first time. Results show that (1) Heatwave exposure is pronounced in eastern China, particularly in Southeast (SE), North China (NC), and Southwest (SW) regions. From 2000 to 2019, heatwave exposure showed an overall upward trend, with the most rapid escalation observed in the SE, NC, and SW regions. Population exposure manifests as a clustered expansion pattern, while GDP exposure demonstrates a more centralized distribution. (2) Climatic factors exert the most notable influence on population exposure, while GDP predominantly impacts economic exposure. The combination of climate and socioeconomic factors contributes less to exposure rates, except in the Northeast (NE) and Southwest (SW) regions where it impacts GDP exposure most. (3) High-risk hotspot cities include Shanghai, Beijing, Chongqing, Guangzhou, Wuhan, Zhengzhou, Hangzhou, Xi'an, Tianjin, and Nanjing. These findings underscore the urgent need for targeted interventions and mitigation strategies in these vulnerable areas.

Keywords: heatwave; socioeconomic exposure; climate change; spatiotemporal distribution; Chinese mainland

check for updates

Academic Editor: Rohinton Emmanuel

Received: 21 November 2024
Revised: 25 December 2024
Accepted: 27 December 2024
Published: 29 December 2024

Citation: Wu, W.; Liu, Q.; Li, H.; Huang, C.; Cheng, W. Mapping Heatwave Socioeconomic Exposure in the Chinese Mainland for the Period of 2000–2019. *Atmosphere* **2025**, *16*, 28. https://doi.org/10.3390/atmos16010028

Copyright: © 2024 by the authors. Licensee MDPI, Basel, Switzerland. This article is an open access article distributed under the terms and conditions of the Creative Commons Attribution (CC BY) license (https://creativecommons.org/licenses/by/4.0/).

1. Introduction

In the context of global warming, the population across the globe has been suffering from extreme weather events in recent years [1,2]. As one of the most harmful extreme weather events [1,3], heatwave events have increased in frequency, intensity, and duration and their impact on human health and the economy has also increased since the 1950s [4,5]. For example, heatwaves that occurred in western North America in 2021 resulted in more than 1400 deaths [6,7], which evidenced that even regions with advanced administrative and medical experience cannot avoid the catastrophic consequences of heatwaves. Indeed, the changes in exposure to heat stress will be critical to heat-related morbidity and mortality [1,8,9]. Therefore, assessment of the spatiotemporal distribution of heatwave exposure is meaningful for residents and policy makers.

Heatwaves, typically defined as prolonged periods of excessive heat lasting more than three days [10], lack a universally accepted definition [11]. Various thermophysiological and heat exchange theories have led to indicators like wet-bulb globe temperature (WBGT) [12] and heat index (HI) [13] that consider factors such as wind speed and relative humidity to evaluate thermal comfort. The thresholds for defining heatwaves include absolute, relative, and combined criteria. Recent studies have shown that combining absolute and relative thresholds enhances the accuracy of defining heatwaves: absolute thresholds provide intuitive clarity, while relative thresholds accommodate spatial climatic heterogeneity effectively [14–16].

Heatwave exposure, measured by the impact on populations and gross domestic product (GDP), has profound implications for health and economies [8]. There is clear evidence that heatwave exposure has far-reaching consequences for human health and the economy [4,17]. Recent research has focused on historical detection and future prediction of heatwave impacts [4,18,19], using tools like Global Heatwave and Warm-Spell Record (GHMR) [20] and scenarios like Shared Socioeconomic Pathways (SSPs) proposed by the Intergovernmental Panel on Climate Change (IPCC) [21]. While the duration of heatwaves is commonly considered in exposure analysis, neglecting frequency and intensity can limit understanding. The HWI (Heatwave Index) is a HI-based definition of the intensity of a heatwave with a minimum duration, while the HHI (heatwave hazard index) is a composite index that takes into account all three of the above heatwave metrics after extracting the heatwave, not just the duration [22], which may give the HHI some advantages as a means of conducting exposure analyses. Therefore, it is crucial to comprehensively analyze the spatial distributions and temporal variations in heatwave exposure, along with the contributions of climate and socioeconomic factors.

Research in the Chinese mainland has advanced in assessing heatwave exposure, such as spatiotemporal assessments by Li and Zha [23] and forecasting studies by Sun et al. [24]. However, existing studies often suffer from small study areas, outdated timeframes, low spatial resolutions, or single-factor analyses. Despite a steady increase in heatwave hazards in China from 2000 to 2019—coinciding with significant economic development and population mobility, especially after joining the World Trade Organization in 2001 and hosting the Beijing Olympics in 2008 [25,26]—a comprehensive national-scale investigation into socioeconomic exposure to heatwaves during the summer months is currently lacking.

This study defined heatwave by the HWI, and then analyzed spatiotemporal distribution of the heatwave historical exposure in the Chinese mainland (hereafter China) for the period 2000–2019 based on HHI as a climate factor, and total and vulnerable population and GDP as socioeconomic factors. After that, we calculated climate and socioeconomic effects and their interaction on exposure. Finally, we determined the aggregate heatwave population exposure (APE) and the aggregate GDP exposure (AGE) and their trends in built-up areas at the city and county levels.

2. Materials and Methods

2.1. Study Drea and Data

China has a large latitudinal and longitudinal span and complex and diverse terrain and climate types [27]. Nationally, the extremely high temperature is concentrated in summer. Due to the combined influence of human activities and natural factors, climate change has led to a significant increase in the frequency and intensity of heatwaves widely observed in China during summer [28–31]; even in the Qinghai–Tibet Plateau, the highest terrain and the coolest place in China, an obvious upward trend was observed [32–35].

Meanwhile, as the largest developing country, China is one of the regions that has suffered most severely from heatwaves due to its large population, rapid urbanization, and

population aging [36–39]. The changes in temperature and populations in different regions of China are different. Therefore, it is divided into six sub-regions, including North China (NC), Southwest (SW), Southeast (SE), Northeast (NE), and Northwest (NW) China and the Tibetan Plateau (TP) according to the social–economic and geo-climatic conditions [40] (Figure 1). To characterize heatwave exposure in China, we utilize the designation "CN" to signify China for subsequent statistical elucidation.

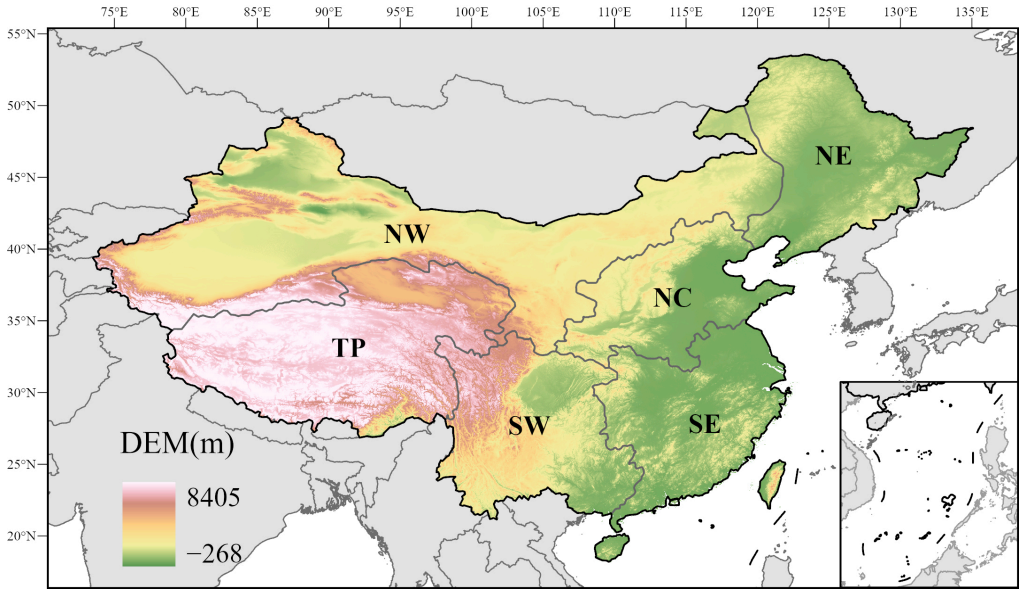


Figure 1. Study area: sub-regions including North China (NC), Southwest (SW), Southeast (SE), Northeast (NE), Northwest (NW) China and the Tibetan Plateau (TP).

In this study, daily grid meteorological datasets were used to calculate annual heatwave records [22]. Elevation, population, and GDP data are bilinearly resampled to the spatial resolution of 0.01°. The elevation data were used in ANUSPLIN model, a spatial interpolation method for meteorological data based on thin-plate smooth spline function theory developed by the Australian National University, and population and GDP were employed as the source of socioeconomic exposure in the assessment of the heatwave.

This study utilized data from various sources: elevation data were sourced from the Resource and Environmental Science and Data Center (RESDC) of the Chinese Academy of Sciences; Population data covering the period 2000–2019 were obtained from the WorldPop research program [41], employing a top-down unconstrained random forest-based dasymetric redistribution method for calculation. Gridded GDP data [42], also from RESDC, were derived using a multi-factor weight assignment method incorporating national sub-county GDP statistics, land use, nightlight data, and settlement density. The Rising LAB [43] index model categorized 337 cities into six tiers based on factors such as commercial concentration, city hubs, activity levels, lifestyle diversity, and future potential. The China Urban Built-up Areas dataset was accessed from A Big Earth Data Platform for Three Poles [44] to focus on densely populated and economically developed areas.

2.2. Method to Calculate Heatwaves

In this study, we used the HWI to identify heatwave events. HWI is derived from the Torridity Index (TI) and HI, a valid index for predicting heatwave weather [13]. TI, calculated

from MT and RH, identifies torridity days when TI meets or exceeds a threshold, TI′. For our analysis, TI′ was determined as the 50th quantile of TI values where MT > 33 °C.

$$\begin{cases} TI = 1.8 \times MT - 0.55 \times (1.8 \times MT - 26) \times (1 - 0.6) + 32, \ RH \leq 60\% \\ TI = 1.8 \times MT - 0.55 \times (1.8 \times MT - 26) \times (1 - RH) + 32, \ RH > 60\% \end{cases} \quad (1)$$

HI incorporates TI and TI′ to quantify the cumulative heat effect, defining a heatwave as a period of 3 or more consecutive torrid days with HWI ≥ 2.8.

$$HI = 1.2 \times (TI - TI') + 0.35 \sum_{i=1}^{N} 1/nd_i (TI_i - TI') + 0.15 \sum_{i=1}^{N-1} 1/nd_i + 1 \quad (2)$$

$$HWI = \sum_{i=1}^{N} HI_i \quad (3)$$

Here, TI_i represents TI of the i-th torridity day before the current day; nd_i represents the number of days from the i-th day before the current day to the current day; HI_i represents the i-th day in a heatwave event; N represents the duration of the heatwave event, and the unit is day (d).

Heatwave frequency (HWF), maximum HI of a heatwave (HWMHI), and maximum heatwave duration (HWMD) in a year—representing frequency, intensity, and duration, respectively—were used to calculate HHI [22]. In this study, the unit of HHI is ha, and the range is normalized to 0–1. And HHI was employed to calculate heatwave exposure as a climatic factor.

$$HHI = (\overline{HWF} + \overline{HWMD} + \overline{HWMHI})/3 \quad (4)$$

2.3. Climate and Socioeconomic Effects on Changes in Heatwave Exposure

Heatwave socioeconomic exposure ($E_{Socioeco}$) contains two aspects: population exposure (E_{Pop}) and GDP exposure (E_{GDP}). Heatwave exposure was usually calculated by multiplying population or GDP with heatwave characteristics (usually duration) in each grid cell each year [9,16,18]. To provide a more comprehensive analysis of heatwave socioeconomic exposure, HHI, a comprehensive index was introduced to calculate exposure.

For a given year (y) and a given grid (g), the heatwave exposure is the product of the climate factor (HHI) and the socioeconomic factor (population, GDP). In this study, E_{Pop} is expressed in person·ha, and E_{GDP} is expressed in CNY·ha.

$$\begin{pmatrix} E_{Pop,\,y,\,g} = HHI_{y,\,g} \times Pop_{y,\,g} \\ E_{GDP,\,y,\,g} = HHI_{y,\,g} \times GDP_{y,g} \end{pmatrix} \quad (5)$$

The changes in $E_{Socioeco}$ are influenced by changes in climate, socioeconomic, and their interactions (Equation (6)), and the contribution of three aspects (C_{HHI}, $C_{Socioeco}$, C_{both}) is analyzed as in Equation (7) [40,45].

$$\Delta e = (h + \Delta h)(s + \Delta s) - h \times s = h \times \Delta s + s \times \Delta h + \Delta h \times \Delta s \quad (6)$$

$$\begin{cases} C_{HHI} = s \times \Delta h/\Delta e \\ C_{Socioeco} = h \times \Delta s/\Delta e \\ C_{both} = \Delta h \times \Delta s/\Delta e \end{cases} \quad (7)$$

Here, h and s respectively represent the values of HHI and socioeconomic factors at the starting period; "Δh", "Δs", and "Δe" are the increases in HHI, socioeconomic factors, and heatwave exposure relative to starting period.

2.4. Other Methods

We conducted temporal trend analysis using least squares linear regression to investigate variations in heatwave exposure and the contributions of climatic and socioeconomic factors. Time points were denoted as "2000–2005", representing variable changes and factor contributions from 2000 to 2005. Time periods like "for5-lat5" denote averages over the first 5 years (2000–2005) compared to the last 5 years (2015–2019). Logarithmic scales were used due to data distribution characteristics, focusing on areas where heatwaves occurred by excluding non-affected regions.

To analyze heatwave exposures across cities by economic development tiers, cities were classified based on index models and intersected with urban built-up area data to refine spatial extents. Statistical analyses were then conducted to assess socioeconomic exposures. Similarly, counties were analyzed from their original extents to mitigate biases from suburban areas in overall statistics.

3. Results

3.1. Spatial Distribution of Socioeconomic Heatwave Exposures

Figure 2a illustrates the spatiotemporal distribution of heatwaves across China from 2000 to 2019 using a normalized HHI, where one represents a maximum hazard and zero indicates a minimal. To distinguish between the severity of low HHI and the occurrence of heatwaves, areas where no heatwave events occurred within the study region were masked. High-hazard areas are concentrated in eastern and northwestern China (e.g., NC, SE, and western NW), with the southeastern TP showing the highest HHI. Line graphs along longitudinal and latitudinal axes show variability in average HHI, highlighting fluctuations along specific geographic corridors. Figure 2b compares HHI across regions, identifying SE and NC as most affected with higher proportions of heatwave events. SE exhibits both frequent and intense heatwaves, while TP experiences fewer occurrences but significant intensity when heatwaves do occur.

Figure 3 illustrates the spatial patterns of socioeconomic factors and their heatwave exposures from 2000 to 2019. GDP distribution (Figure 3a) shows intense concentration in SE, highlighting it as a major economic hub. Population distribution (Figure 3b) mirrors GDP patterns, indicating demographic hotspots in financial centers. Figure 3c,d quantify GDP and population exposure, respectively, with high values in southeastern China like southern and northeastern SE, NC, and northeastern SW, indicating significant socioeconomic vulnerability. Within these areas, GDP exposure demonstrates a more pronounced spatial clustering effect compared to population exposure, exhibiting a trend of diminishing intensity radiating outward from multiple hotspot regions. Although population exposure also features several hotspots, the disparities between these hotspots and surrounding areas are less distinct, highlighting different patterns in the impacts of heatwave hazards on GDP and population. In contrast, in the NE, NW, and TP regions, high-intensity heatwaves do occur in certain parts of the NW and TP; however, these events are typically situated in areas with limited human activity, thereby reducing the exposure in these regions. Moreover, the NE is among the regions in China with lower heatwave hazard, which correspondingly results in lower levels of heatwave exposure.

Figure 3e,f depicts regional disparities: SE emerges as a dominant economic powerhouse with dense population, while TP has minimal economic output and lower population density. Despite economic strength, SE and NC face high GDP exposure, suggesting vulnerability to environmental and economic challenges. Despite larger population and GDP, NE shows comparatively lower exposure, likely due to its higher latitude and reduced heatwave risk.

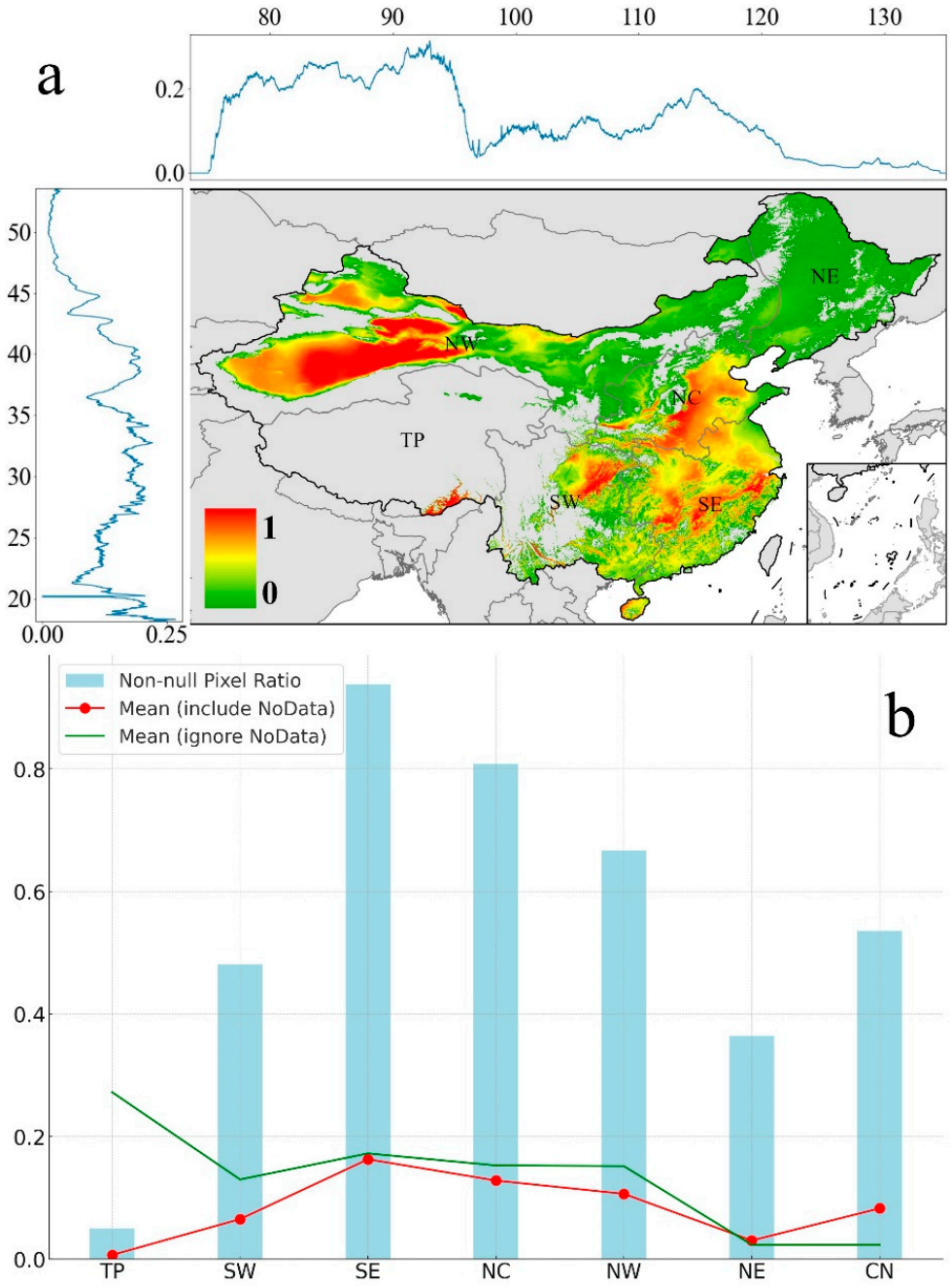


Figure 2. Average HHI (areas where no heatwave occurred were masked) (**a**), Zonal HHI, and Non-null pixel ratio (**b**).

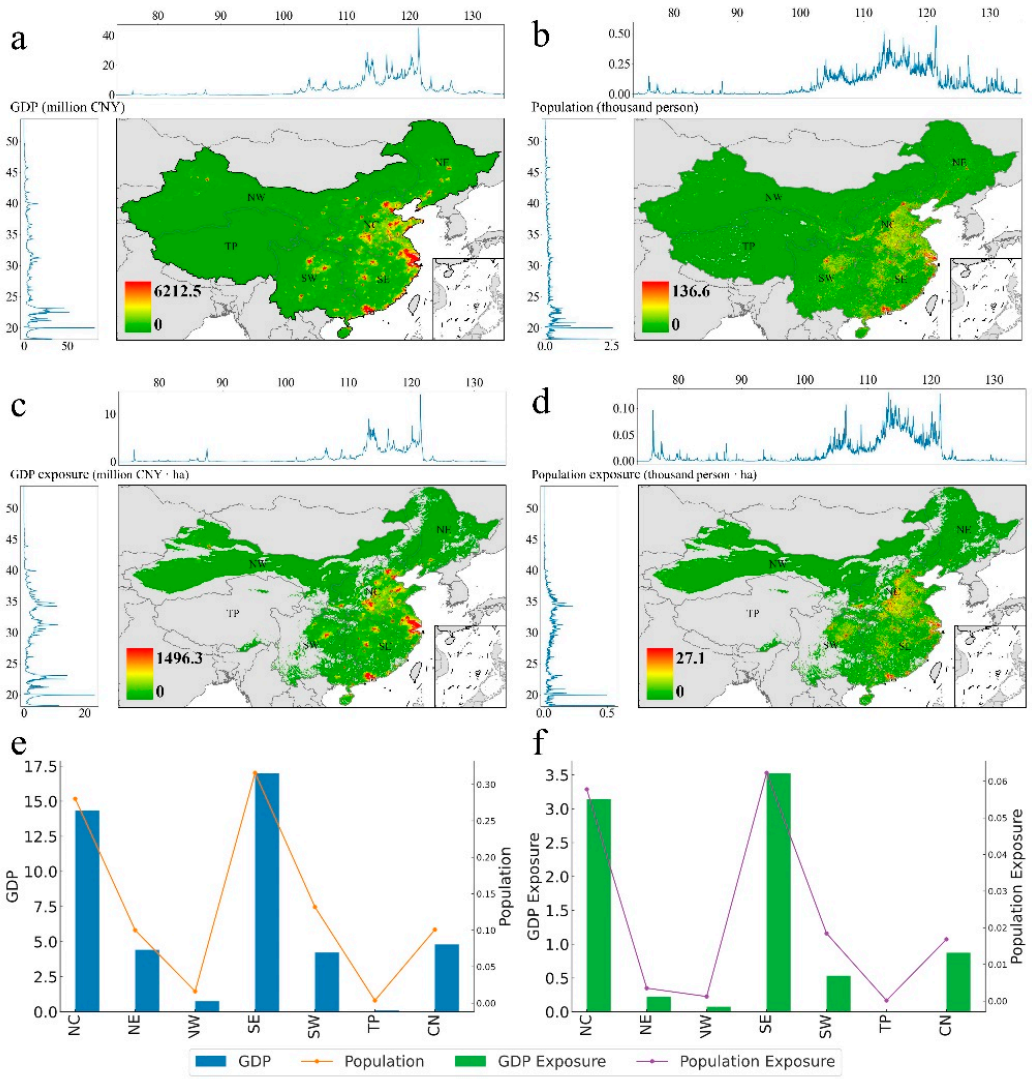


Figure 3. Spatial distribution of Gross Domestic Product (GDP) (million CNY) (**a**), population (thousand person) (**b**), GDP exposure (million CNY·ha) (**c**), population exposure (thousand person·ha) (**d**), zonal mean value of GDP and population (**e**), and zonal mean value of GDP exposure and population exposure (**f**).

3.2. Observed Increasing Trends of Heatwave Exposures

Regression analysis examined temporal variations in heatwave exposures and driving factors, using year as the independent variable and annual averages of exposure as the dependent variable (Figure 4). Narrow confidence intervals in the figures indicate reliable trend estimates.

Nationally, all variables showed increasing trends over the study period. Regionally, disparities in heatwave-related exposures were pronounced. GDP and population trends uniformly rose across all regions, notably in SE, NC, and SW, reflecting robust social development and increased vulnerability to heatwaves. SE, NW, and SW regions also saw rises in HHI, EGDP, and EPop, highlighting the need for enhanced heatwave mitigation strategies. In contrast, TP showed relative stability in heatwave hazard and exposure, likely due to different climatic conditions.

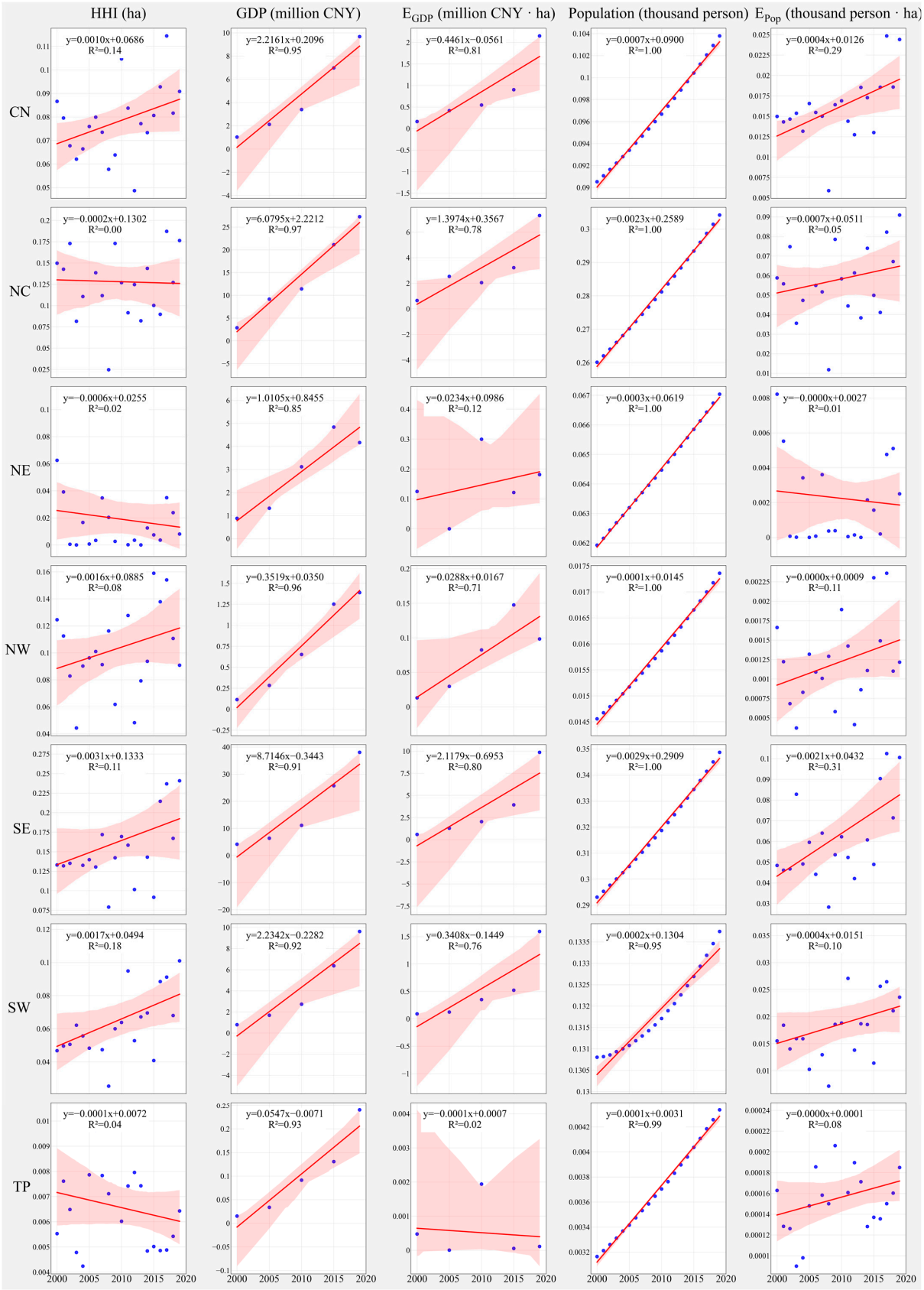


Figure 4. Temporal variations in annual average HHI (ha), GDP (million CNY), E_{GDP} (million CNY·ha), Population (thousand person), E_{Pop} (thousand person·ha) for different regions. E_{GDP} and E_{Pop} represent heatwave exposure of GDP and Population. Observed data are depicted as dots, the fitted model is represented by a line, and the confidence interval is illustrated by the shadows.

Figure 5 integrates economic, demographic, and climatic trends across China, focusing on heatwave exposure. In Figure 5a, GDP growth slopes show robust growth in NC, SE, and northeast SW regions, contrasting with economic decline or stagnation in TP. Figure 5b highlights discrete population growth nodes in urban and urbanizing areas, accompanied by reduced population density in surrounding regions, reflecting accelerated urbanization impacts.

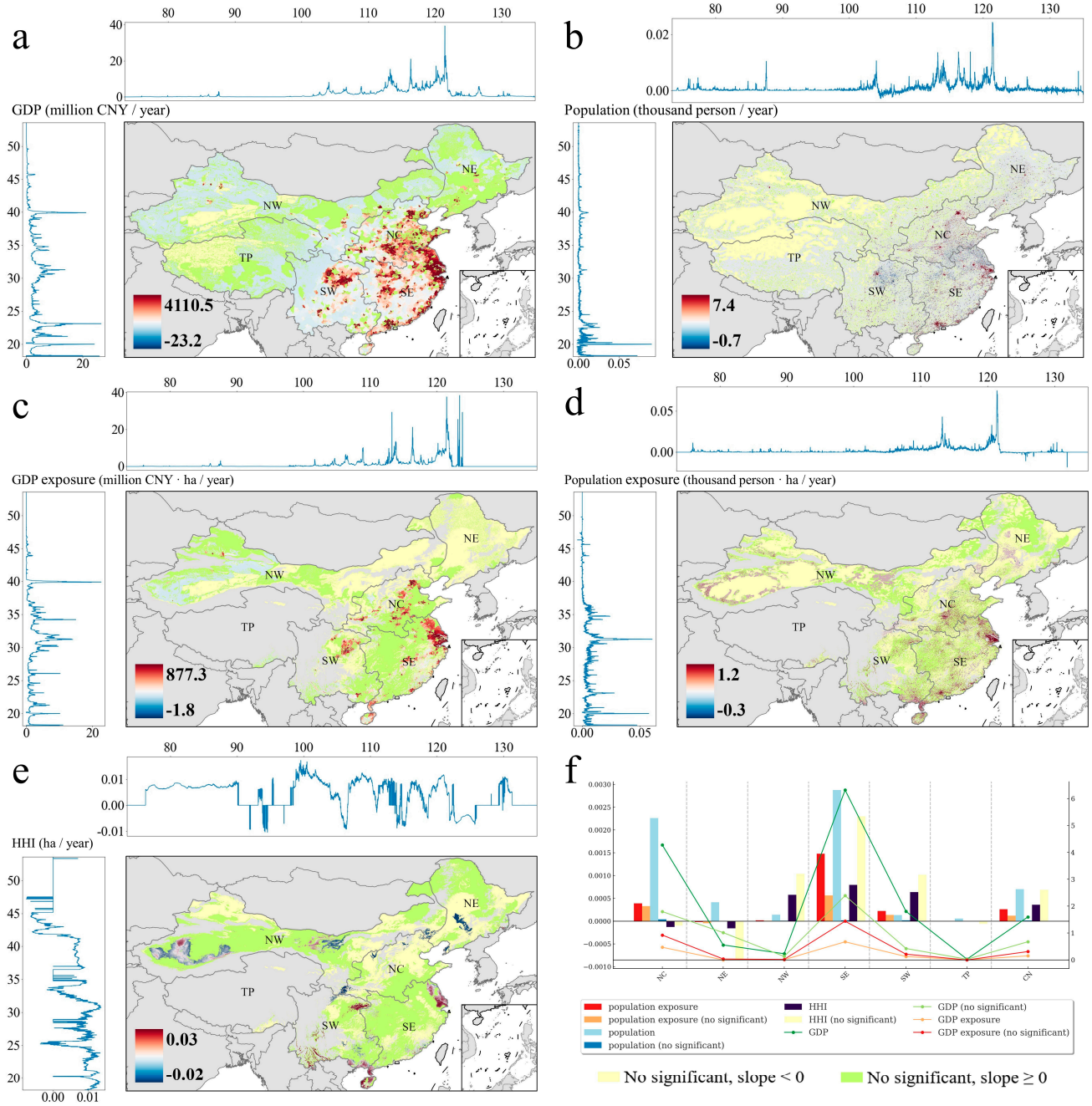


Figure 5. Slope and significance of Gross Domestic Product (GDP) (million CNY/year) (**a**), population (thousand person/year) (**b**), GDP exposure (million CNY·ha/year) (**c**), population exposure (thousand person·ha/year) (**d**), HHI (ha/year) (**e**), and zonal mean value of indices (**f**).

Figure 5c shows GDP exposure in a million CNY per grid per year, concentrated in three main regions: eastern coastal areas around Shanghai, NC, and northeastern SW (including Chengdu and Chongqing). The Pearl River Delta in southern China has a moderate increase in GDP exposure, while NE shows stable or decreasing trends, possibly due to

economic adaptation or lower vulnerability. Figure 5d illustrates population exposure in thousands of persons per grid per year. Driven by urbanization, multi-point concentrated growth is observed in eastern, central, and southern China, with significant increases noted in southern Xinjiang, reflecting both social development and heightened environmental vulnerability in desert regions.

Figure 5e shows a nationwide increase in HHI across China (excluding TP), particularly in eastern, southern, and southwestern regions, growing annually by 0.02 ha. Conversely, northern, northeastern, and northwestern China exhibit decreased HHI, indicating varied heatwave hazards. Lower latitudes generally have higher HHI growth rates. Figure 5f compares variables nationally and regionally. Despite national HHI growth, NC and NE show negative HHI growth. This underscores while some areas show reduced heatwave hazards, social activities sensitive to high temperatures may still face significant risks.

3.3. Contribution Rates of Climate and Socioeconomic Factors to the Exposure

We analyzed changes for different Phase I and Phase II combinations (11 groups in total) separately. We displayed in Figure 6, where we found that from Phase I to Phase II, the magnitude of change in the mean values of different former and latter years is smaller than that of the 2000–2019 period for almost all variables and regions, but in terms of change in the mean values, it can be seen that over different time periods, the regions of heatwave socioeconomic exposure and its impact factor all change positively over time. The maximum values of the changes of all variables occur in the SE region for 2015–2019 (Figure 6a) and 2000–2019 (Figure 6b–e). It is worth mentioning that the SE region, as one of the most economically active regions in China, is highly exposed to the heatwave hazard [46–48]. The increase in exposure in SE amounted to at least 8 million CNY·ha, and at least 40 person·ha each grid, respectively.

Except for the SE region, the socioeconomic exposures of NC, despite experiencing a 2005–2010 decline, showed a strong increasing trend in all other periods, and the opposite was true for NE, where population exposure increased from 2005–2010, but maintained a decline in all other periods, leading to a decline throughout the observation period. In contrast, in the context of minimal population growth (less than 10 people per grid), SW witnessed substantial economic expansion, evidenced by a GDP increase of 10 million CNY. This growth occurred alongside the second-largest variation in HHI, indicating an escalation in socioeconomic exposure. Consequently, apart from SE and NC, the SW area is also increasingly susceptible to heatwave threats. This vulnerability is exacerbated by the region's ongoing socioeconomic development, which, in turn, impedes progress in both population and economic domains due to escalating heatwave impacts.

In this study, we systematically analyzed climate and socioeconomic contributions to heatwave exposure from 2000 to 2019. Figure 7 presents box plots illustrating variations in contribution rates for GDP exposure (Figure 7a) and population exposure (Figure 7b). Each panel depicts different subsets of factors: climate (Figure 7(a1,b1)), socioeconomic (Figure 7(a2,b2)), and their combined effect (Figure 7(a3,b3)).

Climate factor alone (Figure 7(a1)) shows moderate contribution rates with variability across periods for GDP exposure. The influence of GDP alone (Figure 7(a2)) exhibits significant variability, particularly in regions like NE and TP. When considering both climate and GDP factors (Figure 7(a3)), NE and SW show higher median contributions, suggesting a combined impact of climate and economic factors in these regions. Turning to population exposure, the climate factor (Figure 7(b1)) shows minimal median deviation but notable regional variations. The population factor (Figure 7(b2)) highlights increased sensitivity in NC, SE, and NE over the period 2000–2019. The combined effect of climate and population factors (Figure 7(b3)) indicates moderated variability, particularly in NW and

SW. Overall, climate factor dominates changes in population exposure (56–70%), followed by population factors alone, with their combined contribution being the lowest from 2000 to 2019 (Figure 7b).

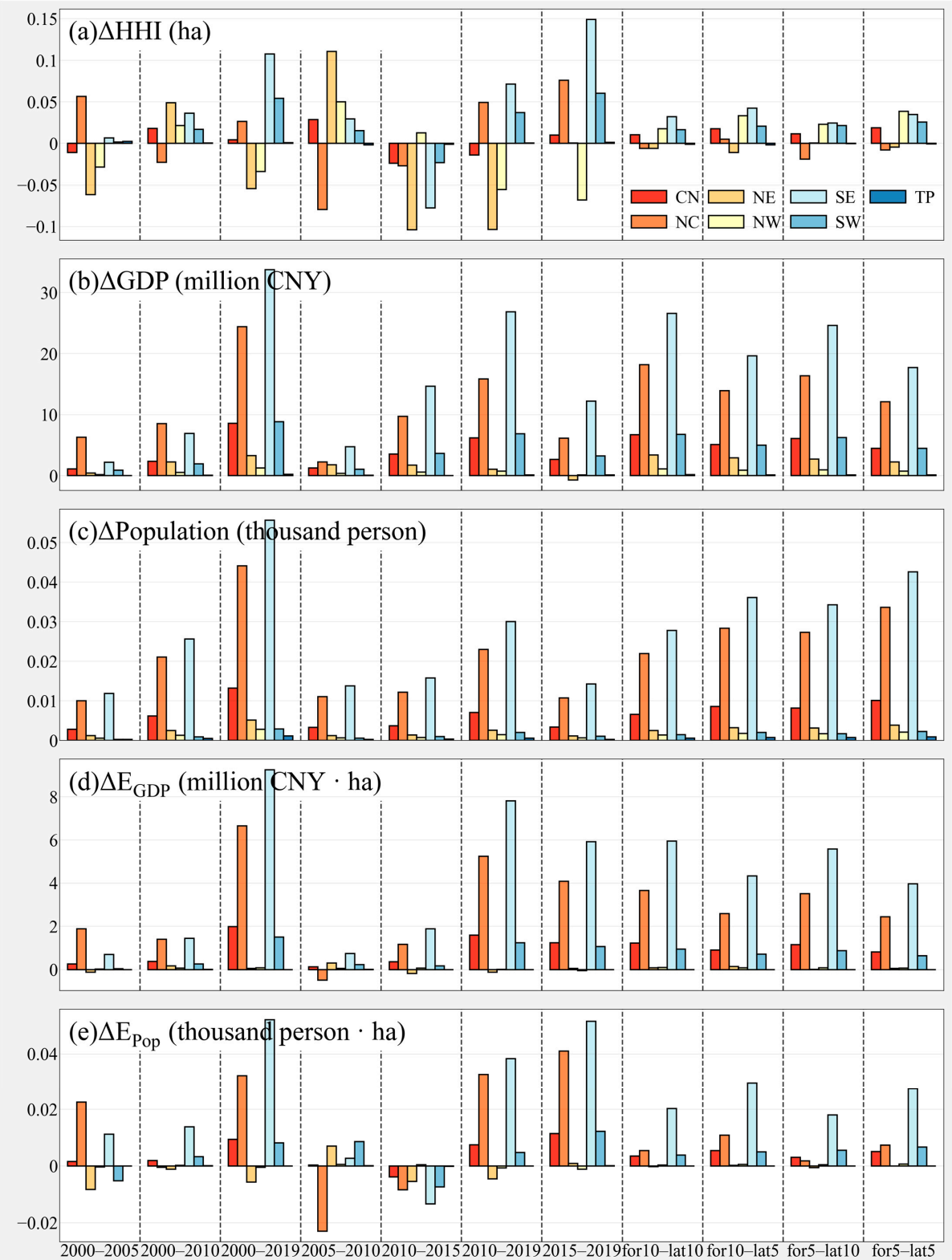


Figure 6. Changes in HHI (**a**), GDP (**b**), Population (**c**), E_{GDP} (**d**), E_{Pop} (**e**) from Phase I (time before "–") to Phase II (time after "–") during the observed period. Different color means different regions.

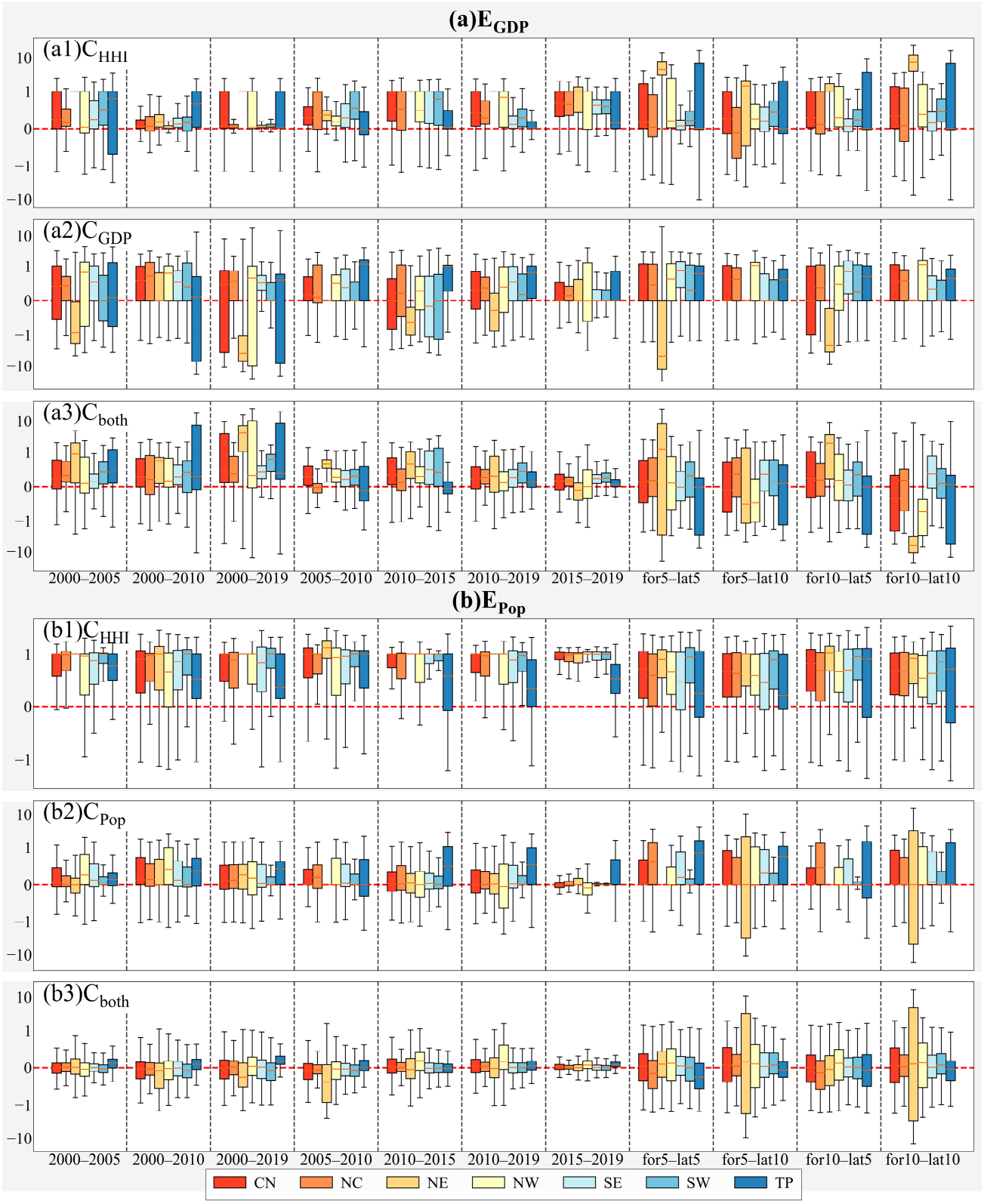


Figure 7. Contribution rates of climate (**a1**,**b1**) and socioeconomic factors (**a2**,**b2**) and their interactions (**a3**,**b3**) to GDP exposure (**a**) and population exposure (**b**).

3.4. Ranking Heatwave Socioeconomic Exposure Levels of China

We assessed APE and AGE values at city and county levels, noting their slopes and significance, and the top 10 units with the fastest increase in each table are presented in bold. Shanghai and Beijing led in APE and AGE, respectively (Tables A1 and A2). Pudong

New District in Shanghai showed the highest APE and AGE, indicating significant regional development (Tables A3 and A4).

The top 10 fastest-growing units consistently ranked among the top 100 in average values across Tables A1–A4, suggesting rapid growth in areas with higher heatwave socioeconomic exposure. Significant units are marked with "*" and "**" for $p < 0.05$ and $p < 0.01$, with 70%, 40%, 90%, and 50% showing significant increases in cities and counties for APE and AGE respectively (Tables A1–A4). Notably, highly significant increases accounted for 57% and 67% of significant increases in city and county APE levels (Tables A1 and A3).

Top first-tier, new first-tier, and second-tier cities by APE include Shanghai, Beijing, Chongqing, Guangzhou, Wuhan, Zhengzhou, Hangzhou, Xi'an, Suzhou, and Tianjin (Table 1). The leading cities for AGE are Shanghai, Beijing, Guangzhou, Shenzhen, Zhengzhou, Wuhan, Suzhou, Foshan, Dongguan, and Hangzhou (Table 2). There is notable overlap with 7 cities appearing in the top 10 for both indicators, expanding to 13 in the top 15 and 17 in the top 20, emphasizing the strong correlation between high population density and economic activity. Among provincial capitals, Shanghai, Beijing, Chongqing, Guangzhou, Wuhan, Zhengzhou, Hangzhou, Xi'an, Tianjin, and Nanjing.

Table 1. APE ranking of first-tier, new first-tier, and second-tier cities.

Index	City	Index	City	Index	City	Index	City
1	** Shanghai	14	Changsha, Hunan	27	Shenyang, Liaoning	40	** Xiamen, Fujian
2	Beijing	15	Shijiazhuang, Hebei	28	* Changzhou, Jiangsu	41	Lanzhou, Gansu
3	Chongqing	16	Shenzhen, Guangdong	29	Nanning, Guangxi	42	Yantai, Shandong
4	* Guangzhou, Guangdong	17	Chengdu, Sichuan	30	Xuzhou, Jiangsu	43	Harbin, Heilongjiang
5	* Wuhan, Hubei	18	Ningbo, Zhejiang	31	** Jiaxing, Zhejiang	44	Quanzhou, Fujian
6	** Zhengzhou, Henan	19	Jinhua, Zhejiang	32	Zhongshan, Guangdong	45	Zhuhai, Guangdong
7	Hangzhou, Zhejiang	20	** Wuxi, Jiangsu	33	* Huizhou, Guangdong	46	* Dalian, Liaoning
8	* Xi'an, Shaanxi	21	Hefei, Anhui	34	Yangzhou, Jiangsu	47	Guiyang, Guizhou
9	** Suzhou, Jiangsu	22	Nanchang, Jiangxi	35	* Nantong, Jiangsu	48	Changchun, Jilin
10	Tianjin, Tianjin	23	Fuzhou, Fujian	36	** Haikou, Hainan	49	* Kunming, Yunnan
11	* Nanjing, Jiangsu	24	** Wenzhou, Zhejiang	37	Taiyuan, Shanxi		
12	Dongguan, Guangdong	25	Shaoxing, Zhejiang	38	Taizhou, Zhejiang		
13	* Foshan, Guangdong	26	Jinan, Shandong	39	Qingdao, Shandong		

Noted: * means $p < 0.05$, ** means $p < 0.01$.

Table 2. AGE ranking of first-tier, new first-tier, and second-tier cities.

Index	City	Index	City	Index	City	Index	City
1	* Shanghai	14	* Wuxi, Jiangsu	27	* Shaoxing, Zhejiang	40	Harbin, Heilongjiang
2	* Beijing	15	Nanjing, Jiangsu	28	Yangzhou, Jiangsu	41	Lanzhou, Gansu
3	Guangzhou, Guangdong	16	Changsha, Hunan	29	* Nantong, Jiangsu	42	* Taizhou, Zhejiang

Table 2. *Cont.*

Index	City	Index	City	Index	City	Index	City
4	Shenzhen, Guangdong	17	* Ningbo, Zhejiang	30	** Jiaxing, Zhejiang	43	Yantai, Shandong
5	Zhengzhou, Henan	18	Shijiazhuang, Hebei	31	Jinhua, Zhejiang	44	Qingdao, Shandong
6	Wuhan, Hubei	19	* Changzhou, Jiangsu	32	* Wenzhou, Zhejiang	45	Quanzhou, Fujian
7	** Suzhou, Jiangsu	20	Jinan, Shandong	33	Xiamen, Fujian	46	Dalian, Liaoning
8	Foshan, Guangdong	21	Fuzhou, Fujian	34	Taiyuan, Shanxi	47	* Kunming, Yunnan
9	Dongguan, Guangdong	22	Hefei, Anhui	35	* Nanning, Guangxi	48	Changchun, Jilin
10	* Hangzhou, Zhejiang	23	Shenyang, Liaoning	36	Chengdu, Sichuan	49	Guiyang, Guizhou
11	Tianjin, Tianjin	24	Zhongshan, Guangdong	37	Huizhou, Guangdong		
12	* Xi'an, Shaanxi	25	* Nanchang, Jiangxi	38	** Haikou, Hainan		
13	Chongqing	26	Xuzhou, Jiangsu	39	Zhuhai, Guangdong		

Noted: * means $p < 0.05$, ** means $p < 0.01$.

4. Discussion

Our study on heatwave exposure in China aligns with global and regional findings [22,49]. Regions like NE and SW show higher exposure due to combined climate and GDP factors, which could be correlated with the economic structure or the concentration of wealth in these areas [50]. Temporally, population exposure rates are declining, emphasizing climatic influences [19,51]. In fact, their coarse resolution (more than 10 km) is not enough to describe the exposure in the build-up regions. By contrast, the present study improves the data to 0.01°, which helps to reflect the finer spatial difference.

In other ways, we differ somewhat from previous studies. Our approach introduced HHI, integrating absolute and relative thresholds to comprehensively define heatwaves. Unlike traditional methods, which rely on heatwave days alone [49,52], HHI considers intensity, frequency, and duration, offering a nuanced portrayal of heatwave characteristics. This methodological advancement is crucial for accurately assessing heatwave impacts on human health and infrastructure resilience.

On a national scale, eastern China faced the highest and rapidly increasing heatwave risks attributed to climate and socioeconomic factors [22], particularly in socioeconomically active regions like SE. The concentration of both economic and human resources in the SE necessitates targeted heatwave preparedness strategies to safeguard against the detrimental impacts of such events [16,40,53]. For example, local governments in the region should pay attention to the construction of places for outdoor workers to avoid the heat in urban planning, and establish appropriate early warning mechanisms for high temperatures, as well as matching work systems and regulations, etc. Individuals should also pay attention to the temperature situation and take effective measures to prevent heatstroke. This regional discrepancy suggests underlying demographic shifts, possibly migration from less urbanized to more urbanized areas. TP shows widespread population growth, likely driven by economic activities or natural increases. Conversely, NE exhibits all statistical measures entrenched in negative values, indicating significant population outflow from this region [54].

Regarding GDP exposure relative to population exposure, NE and NW show no significant changes over time, likely due to stable economic and demographic development [55,56]. TP, characterized by limited low-altitude areas in the southwest, experiences minimal changes in heatwave exposure but faces increasing risks due to global warming trends, threatening environmental stability [57–59].

GDP exerts a significant influence on exposure but is moderated by climate factors. In China, climate and combined climate–population factors positively contribute to heatwave exposure, while GDP shows a negative impact (Figure 7a). This suggests that increasing GDP correlates with reduced heatwave exposure, potentially linked to China's recent efforts towards carbon neutrality [60,61]. The detailed analysis underscores the complex interactions shaping heatwave exposure. The interplay between climate conditions and socioeconomic factors like GDP and population highlights the multifaceted nature of heatwave risks. Different regions show varying susceptibilities to economic and demographic changes, influenced by climate variability [62,63]. This complexity emphasizes the need for tailored strategies that address the diverse dimensions of heatwave risks through effective mitigation and adaptation measures.

There are several study limitations to consider. Introducing the HHI provides a holistic view but raises questions about the optimal method for capturing the diverse nature of heatwaves. Moreover, the presence of null values in calculations introduces ambiguity due to varied computational methods. Excluding regions without recorded heatwave events from the statistical analysis could lead to underestimation or overestimation of regional data compared to other studies, necessitating refined approaches for constructing the Heatwave Hazard Index. Meanwhile, resampling socioeconomic data from 1 km to 0.01° at different latitudes may introduce some loss of precision, which may impose some limitations on the accuracy of the results, and better up-scaling methods should be considered in future relevant studies.

Vulnerable populations, including those with cardiovascular and respiratory conditions, and older adults, face heightened heatwave risks [8,64,65], significantly surpassing global averages [66]. Nighttime heatwave studies are gaining attention [67–69]. Global climate change and urbanization compound these risks, with the urban heat island effect amplifying heatwave impacts globally [70–72]. Compounded climate extremes such as droughts, floods, and heatwaves pose challenges to agricultural productivity and socio-environmental sustainability [73,74]. Future research should prioritize studying these vulnerable populations and compounded factors.

Overall, the results suggest that the population and GDP of the study region are highly vulnerable to heatwave hazards. As an engine of China's economic and social development, SE, NC, and SW are facing an increasing threat of heatwaves. Although NE and NW have less change in heatwave exposure under the influence of economic development and population mobility, attention should be paid to the threat of heatwaves in their urbanization process. Based on our results, future research should pay particular attention to the increasing heat island effect due to poor urban planning, as well as to the compound heatwave hazard and the vulnerable population and economic development in these areas. In addition, the combined effects of socioeconomic and climatic factors on heatwave exposure are becoming greater, which highlights the need for sustainable urban development planning, greenhouse gas mitigation, and appropriate measures to minimize human and economic exposure to heatwaves in the Chinese development process.

5. Conclusions

The adoption of HWI and HHI in this study provides a nuanced characterization of heatwaves, with GDP and population as critical socioeconomic factors. This underscores

the role of climate and socioeconomic factors in shaping heatwave exposure in China. The main conclusions can be summarized as follows:

(a) Significant spatial heterogeneity exists in socioeconomic exposure across China. Eastern regions, particularly SE, NC, and NE SW, exhibit the highest and fastest-growing heatwave exposure due to vigorous economic activity. Temporally, there is an overall increasing trend in heatwave socioeconomic exposure from 2000 to 2019, with SE, NC, and SW showing the most rapid growth in exposure. Population exposure growth shows a multi-point clustered distribution, contrasting with the concentrated distribution of GDP exposure growth.

(b) Factors contribute differently to changes in GDP and population exposure. Nationally, GDP, climate factors, and their combination are primary drivers of economic exposure. Regionally, combinations dominate in NE and SW. For population exposure, climate factors exert the most influence, followed by population factors alone, with combinations having the least impact. NE and TP show higher contributions from population and combinations.

(c) The top 10 provincial capitals with the highest heatwave socioeconomic exposure include Shanghai, Beijing, Chongqing, Guangzhou, Wuhan, Zhengzhou, Hangzhou, Xi'an, Tianjin, and Nanjing.

There is an urgent need for preventive strategies to reduce greenhouse gas emissions and to implement sustainable urban demographic and social development planning in the above regions, especially hotspots in order to minimize socioeconomic hazards under climate change in the face of heatwave exposure.

Author Contributions: Conceptualization, W.W.; Data curation, W.W. and H.L.; Formal analysis, Q.L. and H.L.; Funding acquisition, Q.L. and W.C.; Investigation, W.W.; Methodology, W.W.; Project administration, Q.L.; Resources, Q.L. and C.H.; Software, W.W.; Supervision, Q.L.; Validation, W.W. and H.L.; Visualization, W.W.; Writing—original draft, W.W.; Writing—review & editing, Q.L., H.L. and C.H. All authors have read and agreed to the published version of the manuscript.

Funding: This research was funded by the Innovation Project of LREIS (Project no. KPI008), the Strategic Priority Research Program of the Chinese Academy of Sciences (Category B, Geographic Intelligence, no. XDB0740300), and the Strategic Priority Research Program of the Chinese Academy of Sciences (Project No. XDA20030302).

Institutional Review Board Statement: Not applicable.

Informed Consent Statement: Not applicable.

Data Availability Statement: The data presented in this study are available on request from the corresponding author. The data are not publicly available due to privacy.

Acknowledgments: Thanks are due to Xin Dai and Xilin Wu for valuable discussion.

Conflicts of Interest: The authors declare that they have no known competing financial interests or personal relationships that could have appeared to influence the work reported in this paper.

Appendix A

Table A1. APE ranking of cities (thousand person·ha).

Index	City	Mean	Slope	Index	City	Mean	Slope
1	**** Shanghai,**	2258.088	**224.623**	51	Zhenjiang, Jiangsu	199.119	7.371
2	**Beijing,**	2051.135	**62.409**	52	Zhuzhou, Hunan	196.232	3.007
3	**Chongqing,**	1979.879	**49.056**	53	* Huizhou, Guangdong	193.569	11.382
4	*** Guangzhou, Guangdong**	1332.409	**79.198**	54	Xuchang, Henan	188.428	2.143
5	*** Wuhan, Hubei**	1242.755	**50.731**	55	Yangzhou, Jiangsu	188.339	5.754

Table A1. *Cont.*

Index	City	Mean	Slope	Index	City	Mean	Slope
6	** **Zhengzhou, Henan**	1134.124	**42.675**	56	* Nantong, Jiangsu	186.246	13.722
7	Hangzhou, Zhejiang	1098.011	28.188	57	Jiaozuo, Henan	185.441	3.276
8	* Xi'an, Shaanxi	1029.313	31.811	58	Shantou, Guangdong	185.136	6.304
9	** **Suzhou, Jiangsu**	997.072	**84.431**	59	Xianyang, Shaanxi	183.985	3.514
10	Tianjin, Tianjin	940.835	33.539	60	Fuyang, Anhui	183.766	1.743
11	* Nanjing, Jiangsu	874.412	36.318	61	Wuhu, Anhui	183.437	1.309
12	Dongguan, Guangdong	842.763	29.695	62	Kaifeng, Henan	181.754	3.100
13	* **Foshan, Guangdong**	795.933	**53.404**	63	Baoji, Shaanxi	179.104	1.336
14	Changsha, Hunan	776.707	11.842	64	Yichang, Hubei	174.637	2.229
15	Shijiazhuang, Hebei	675.982	4.146	65	Xingtai, Hebei	170.246	0.183
16	**Shenzhen, Guangdong**	661.249	**36.922**	66	Zhumadian, Henan	168.909	2.119
17	Chengdu, Sichuan	652.318	−2.172	67	Changde, Hunan	164.962	3.075
18	Ningbo, Zhejiang	612.580	20.516	68	Huzhou, Zhejiang	164.597	6.302
19	Jinhua, Zhejiang	568.015	8.150	69	Liaocheng, Shandong	164.496	1.138
20	** **Wuxi, Jiangsu**	559.915	**40.799**	70	Xiangtan, Hunan	163.202	2.249
21	Hefei, Anhui	544.250	10.332	71	Jieyang, Guangdong	162.451	4.666
22	Nanchang, Jiangxi	523.819	15.210	72	Jiangmen, Guangdong	160.791	7.564
23	Fuzhou, Fujian	522.523	11.506	73	Taizhou, Jiangsu	154.782	8.684
24	** Wenzhou, Zhejiang	461.785	30.907	74	** Haikou, Hainan	154.486	12.615
25	Shaoxing, Zhejiang	458.643	5.740	75	Zhoukou, Henan	152.966	2.877
26	Jinan, Shandong	440.830	−0.205	76	Heze, Shandong	150.138	4.196
27	Shenyang, Liaoning	400.188	11.784	77	Xiangyang, Hubei	147.959	−0.535
28	* Changzhou, Jiangsu	389.053	21.510	78	Taiyuan, Shanxi	141.580	4.037
29	Luoyang, Henan	372.312	3.603	79	Taizhou, Zhejiang	139.186	6.977
30	Weifang, Shandong	346.848	3.838	80	Maanshan, Anhui	138.658	0.158
31	* Ganzhou, Jiangxi	333.987	9.318	81	Binzhou, Shandong	137.481	−0.580
32	Nanning, Guangxi	326.584	13.932	82	Dongying, Shandong	135.167	2.552
33	Handan, Hebei	325.405	4.199	83	Cangzhou, Hebei	134.394	−0.963
34	Xuzhou, Jiangsu	323.390	4.864	84	Suzhou, Anhui	130.049	1.783
35	Anyang, Henan	302.602	4.551	85	Huangshi, Hubei	129.248	2.188
36	Zibo, Shandong	280.687	1.825	86	Dezhou, Shandong	129.092	−0.341
37	** Jiaxing, Zhejiang	274.750	17.293	87	Xiaogan, Hubei	127.077	1.870
38	* Xinxiang, Henan	266.132	6.177	88	Jian, Jiangxi	125.635	2.848
39	Baoding, Hebei	256.170	−1.095	89	Luohe, Henan	123.405	3.197
40	Tangshan, Hebei	250.187	−1.857	90	Dazhou, Sichuan	123.236	4.599
41	Zhongshan, Guangdong	248.705	9.682	91	Shangrao, Jiangxi	122.860	2.495
42	Urumqi, Xinjiang	247.201	14.201	92	* Yueyang, Hunan	122.071	5.167
43	Jining, Shandong	244.407	4.846	93	Fuzhou, Jiangxi	119.190	2.432
44	Linyi, Shandong	239.063	2.395	94	* Huaian, Jiangsu	118.684	7.886
45	Nanchong, Sichuan	233.189	5.817	95	Bengbu, Anhui	118.301	−0.138
46	Hengyang, Hunan	233.047	3.372	96	Linfen, Shanxi	117.865	0.822
47	Nanyang, Henan	228.271	5.674	97	* Huaibei, Anhui	115.655	3.904
48	Liuzhou, Guangxi	218.712	4.019	98	Yuncheng, Shanxi	114.963	0.086
49	Mianyang, Sichuan	207.870	1.029	99	Puyang, Henan	113.076	2.262
50	Pingdingshan, Henan	206.766	2.098	100	Langfang, Hebei	113.019	0.695

Note: * means $p < 0.05$, ** means $p < 0.01$; the top 10 cities in terms of APE increase are given in bold; unit of Mean, Slope is thousand person·ha, thousand person·ha/year, respectively.

Table A2. AGE ranking of cities (million CNY·ha).

Index	City	Mean	Slope	Index	City	Mean	Slope
1	* **Shanghai,**	2600.355	**318.023**	51	Pingdingshan, Henan	65.610	5.284
2	* **Beijing,**	2267.727	**326.328**	52	Dongying, Shandong	63.966	1.692
3	**Guangzhou, Guangdong**	1538.518	**222.985**	53	Wuhu, Anhui	63.763	4.274

Table A2. *Cont.*

Index	City	Mean	Slope	Index	City	Mean	Slope
4	**Shenzhen, Guangdong**	912.061	**149.387**	54	** Taizhou, Jiangsu	63.233	8.439
5	**Zhengzhou, Henan**	877.589	**113.516**	55	Yichang, Hubei	60.611	8.116
6	**Wuhan, Hubei**	842.243	**152.994**	56	Zhuzhou, Hunan	59.228	6.856
7	** **Suzhou, Jiangsu**	799.626	**87.783**	57	Chengdu, Sichuan	58.307	−1.957
8	**Foshan, Guangdong**	769.993	**102.483**	58	Puyang, Henan	57.309	4.838
9	**Dongguan, Guangdong**	744.187	**100.092**	59	Jining, Shandong	55.132	5.669
10	* Hangzhou, Zhejiang	732.994	75.359	60	Huangshi, Hubei	55.027	7.406
11	Tianjin, Tianjin	723.944	84.485	61	** Xianyang, Shaanxi	54.892	5.803
12	*** Xi'an, Shaanxi**	637.138	**91.901**	62	Hengyang, Hunan	54.860	7.733
13	Chongqing, Chongqing	543.415	79.415	63	Jiangmen, Guangdong	52.898	5.545
14	* Wuxi, Jiangsu	532.493	64.775	64	Huizhou, Guangdong	50.489	6.518
15	Nanjing, Jiangsu	498.534	68.813	65	* Kaifeng, Henan	50.319	4.926
16	Changsha, Hunan	412.337	53.015	66	Cangzhou, Hebei	50.076	3.952
17	* Ningbo, Zhejiang	359.505	29.662	67	Xiangtan, Hunan	50.012	6.797
18	Shijiazhuang, Hebei	356.421	31.045	68	** Haikou, Hainan	49.207	5.901
19	* Changzhou, Jiangsu	297.441	29.641	69	Yueyang, Hunan	49.189	9.026
20	Urumqi, Xinjiang	280.437	37.136	70	Xingtai, Hebei	48.591	3.992
21	Jinan, Shandong	262.957	29.111	71	Binzhou, Shandong	46.738	3.027
22	Fuzhou, Fujian	245.380	33.105	72	Zhuhai, Guangdong	44.350	7.642
23	Hefei, Anhui	241.732	35.281	73	Huaian, Jiangsu	43.577	6.293
24	Shenyang, Liaoning	239.438	31.245	74	Zhangzhou, Fujian	43.123	6.962
25	Luoyang, Henan	208.839	17.026	75	* Langfang, Hebei	40.253	4.081
26	Zhongshan, Guangdong	185.664	22.807	76	* Mianyang, Sichuan	38.693	5.204
27	* Nanchang, Jiangxi	174.530	20.684	77	* Jieyang, Guangdong	38.531	4.320
28	Xuzhou, Jiangsu	171.905	25.354	78	Maanshan, Anhui	38.300	1.746
29	* Zibo, Shandong	163.281	12.440	79	Dezhou, Shandong	37.969	4.228
30	* Shaoxing, Zhejiang	141.812	8.434	80	* Panzhihua, Sichuan	36.940	4.984
31	* Xinxiang, Henan	119.803	11.913	81	** Huzhou, Zhejiang	35.341	3.150
32	Yangzhou, Jiangsu	113.172	8.588	82	Changde, Hunan	34.907	5.950
33	* Nantong, Jiangsu	108.497	16.027	83	* Zhanjiang, Guangdong	34.674	5.319
34	** Jiaxing, Zhejiang	107.659	9.442	84	Zhaoqing, Guangdong	33.447	4.902
35	Liuzhou, Guangxi	106.640	14.660	85	* Ganzhou, Jiangxi	32.461	3.767
36	Handan, Hebei	105.442	3.895	86	Bengbu, Anhui	32.111	2.746
37	Jinhua, Zhejiang	103.390	4.904	87	Guilin, Guangxi	31.747	5.369
38	Anyang, Henan	102.969	9.122	88	* Heze, Shandong	31.022	3.525
39	Weifang, Shandong	102.104	8.727	89	* Zhoukou, Henan	30.685	2.644
40	* Wenzhou, Zhejiang	101.315	12.300	90	Karamay, Xinjiang	30.651	1.822
41	* Baoding, Hebei	92.912	5.239	91	Harbin, Heilongjiang	30.382	−0.660
42	Xiamen, Fujian	88.966	18.304	92	Lanzhou, Gansu	30.140	1.650
43	Zhenjiang, Jiangsu	88.627	7.078	93	Huaibei, Anhui	29.919	3.564
44	Taiyuan, Shanxi	88.377	7.748	94	Beihai, Guangxi	28.589	5.117
45	Tangshan, Hebei	84.989	7.148	95	* Taizhou, Zhejiang	28.587	3.049
46	Xuchang, Henan	83.336	8.002	96	Liaoyang, Liaoning	28.545	3.082
47	* Shantou, Guangdong	81.471	9.875	97	Liaocheng, Shandong	28.289	1.881
48	Linyi, Shandong	76.239	7.904	98	* Chaozhou, Guangdong	28.127	3.248
49	* Nanning, Guangxi	75.720	9.455	99	Panjin, Liaoning	27.762	1.020
50	Jiaozuo, Henan	72.136	7.227	100	Luohe, Henan	27.447	1.906

Note: * means $p < 0.05$, ** means $p < 0.01$; the top 10 cities in terms of AGE increase are given in bold; unit of Mean, Slope is million CNY·ha, million CNY·ha/year, respectively.

Table A3. APE ranking of counties (thousand person·ha).

Index	County	Mean	Slope	Index	County	Mean	Slope
1	**** Pudong New District, Shanghai**	473.178	**52.180**	51	* Liwan District, Guangzhou, Guangdong	136.747	8.228
2	**Chaoyang District, Beijing**	472.633	**15.341**	52	* Qiaokou District, Wuhan, Hubei	136.134	6.133
3	**** Jinshui District, Zhengzhou, Henan**	395.140	**15.137**	53	** Gusu District, Suzhou, Jiangsu	135.984	11.990
4	Haidian District, Beijing	390.696	11.270	54	Yanta District, Xi'an, Shaanxi	135.255	3.679
5	*** Nanhai District, Foshan, Guangdong**	337.868	**22.894**	55	* Zhanggong District, Ganzhou, Jiangxi	134.542	4.029
6	Fengtai District, Beijing	283.885	9.020	56	Wucheng District, Jinhua, Zhejiang	133.943	2.781
7	*** Shunde District, Foshan, Guangdong**	270.315	**17.302**	57	** Xuhui District, Shanghai	133.426	12.844
8	**** Minhang District, Shanghai**	261.311	**23.018**	58	Longgang District, Shenzhen, Guangdong	132.493	7.389
9	* Baiyun District, Guangzhou, Guangdong	245.558	14.908	59	Zhangdian District, Zibo, Shandong	132.252	0.716
10	Yubei District, Chongqing	240.110	5.993	60	Jianxi District, Luoyang, Henan	131.552	1.020
11	Wuchang District, Wuhan, Hubei	219.999	8.663	61	Shushan District, Hefei, Anhui	131.126	3.008
12	Hongshan District, Wuhan, Hubei	215.713	8.294	62	Gongshu District, Hangzhou, Zhejiang	130.567	3.242
13	Baoan District, Shenzhen, Guangdong	211.695	13.163	63	* Lucheng District, Wenzhou, Zhejiang	130.271	6.865
14	**** Baoshan District, Shanghai**	211.427	**22.510**	64	Yaohai District, Hefei, Anhui	129.220	2.100
15	Shapingba District, Chongqing	210.219	5.126	65	Donghu District, Nanchang, Jiangxi	128.363	3.686
16	Yuhua District, Changsha, Hunan	208.362	2.920	66	Xinhua District, Shijiazhuang, Hebei	127.687	0.555
17	**** Wuzhong District, Suzhou, Jiangsu**	206.143	**18.681**	67	Xixiangtang District, Nanning, Guangxi	127.207	5.173
18	* Haizhu District, Guangzhou, Guangdong	203.525	12.311	68	* Wujin District, Changzhou, Jiangsu	126.553	7.155
19	Jiulongpo District, Chongqing	201.504	4.479	69	* Jiangan District, Wuhan, Hubei	126.353	5.417
20	Xiaoshan District, Hangzhou, Zhejiang	196.696	5.289	70	** Liangxi District, Wuxi, Jiangsu	126.182	9.200
21	Binhai New District, Tianjin	188.376	7.920	71	Yuhua District, Shijiazhuang, Hebei	123.533	0.806
22	** Kunshan, Suzhou, Jiangsu	187.672	15.037	72	Qingshanhu District, Nanchang, Jiangxi	123.425	3.336
23	Yiwu City, Jinhua, Zhejiang	187.310	1.927	73	Xihu District, Hangzhou, Zhejiang	122.811	3.191
24	* Weiyang District, Xi'an, Shaanxi	178.527	5.827	74	Chang'an District, Shijiazhuang, Hebei	122.096	0.778
25	**** Putuo District, Shanghai**	173.974	**17.796**	75	* Jianghan District, Wuhan, Hubei	120.200	5.179
26	** Zhongyuan District, Zhengzhou, Henan	173.749	6.259	76	Keqiao District, Shaoxing, Zhejiang	119.877	2.124

Table A3. *Cont.*

Index	County	Mean	Slope	Index	County	Mean	Slope
27	* Beilin District, Xi'an, Shaanxi	169.248	5.561	77	Daxing District, Beijing	119.503	4.110
28	Yuecheng District, Shaoxing, Zhejiang	168.409	2.337	78	Fucheng District, Mianyang, Sichuan	118.388	0.652
29	Jiangbei District, Chongqing	167.741	3.393	79	Yinzhou District, Ningbo, Zhejiang	116.801	3.870
30	* Panyu District, Guangzhou, Guangdong	165.442	9.997	80	* Chancheng District, Foshan, Guangdong	116.719	7.982
31	* Gulou District, Nanjing, Jiangsu	164.786	6.890	81	Rencheng District, Jining, Shandong	116.615	2.362
32	** Songjiang District, Shanghai	164.546	13.254	82	Baohu District, Hefei, Anhui	116.047	2.638
33	Qiaoxi District, Shijiazhuang, Hebei	163.595	0.899	83	Jinan District, Fuzhou, Fujian	115.759	2.382
34	Xicheng District, Beijing	163.232	5.100	84	Dongcheng District, Beijing	113.668	3.763
35	Wangcheng District, Changsha, Hunan	163.165	2.750	85	Gulou District, Fuzhou, Fujian	113.403	1.817
36	Jianggan District, Hangzhou, Zhejiang	156.939	4.104	86	* Huicheng District, Huizhou, Guangdong	111.643	6.899
37	Qinhuai District, Nanjing, Jiangsu	155.355	6.140	87	Banan District, Chongqing	111.290	2.292
38	Nanan District, Chongqing	154.848	3.741	88	Kaifu District, Changsha, Hunan	111.164	1.603
39	* Yuexiu District, Guangzhou, Guangdong	154.348	9.127	89	** Changshu District, Suzhou, Jiangsu	110.487	8.662
40	Changping District, Beijing	154.197	4.036	90	Haishu District, Ningbo, Zhejiang	109.749	3.350
41	Yuzhong District, Chongqing	152.904	3.098	91	Tiexi District, Shenyang, Liaoning	109.086	3.750
42	Yuhang District, Hangzhou, Zhejiang	150.265	4.457	92	Shunqing District, Nanchong, Sichuan	108.939	2.951
43	* Tianhe District, Guangzhou, Guangdong	149.996	8.691	93	Jiangxia District, Wuhan, Hubei	108.814	3.847
44	* Lianhu District, Xi'an, Shaanxi	149.873	5.137	94	** Jing'an District, Shanghai	108.615	11.327
45	* Xincheng District, Xi'an, Shaanxi	146.671	4.824	95	* Hanyang District, Wuhan, Hubei	108.463	4.659
46	**** Yangpu District, Shanghai**	146.356	**15.778**	96	** Jiangyin District, Wuxi, Jiangsu	106.284	9.174
47	** Jiading District, Shanghai	146.329	13.648	97	Xiacheng District, Hangzhou, Zhejiang	106.085	2.972
48	Cixi City, Ningbo, Zhejiang	145.407	4.256	98	Cangshan District, Fuzhou, Fujian	104.500	2.056
49	** Guanchenghuizi District, Zhengzhou, Henan	144.373	5.518	99	Weidu, Xuchang, Henan	103.683	1.310
50	** Erqi District, Zhengzhou, Henan	140.498	5.533	100	Lianchi, Baoding, Hebei	102.900	−0.369

Note: * means $p < 0.05$, ** means $p < 0.01$; the top 10 counties in terms of APE increase are given in bold; unit of Mean, Slope is thousand person·ha, thousand person·ha/year, respectively.

Table A4. AGE ranking of counties (million CNY·ha).

Index	County	Mean	Slope	Index	County	Mean	Slope
1	*** Pudong New District, Shanghai**	718.968	**97.487**	51	Yuzhong District, Chongqing	102.228	19.133
2	*** Chaoyang District, Beijing**	622.394	**91.499**	52	* Zhangdian District, Zibo, Shandong	99.562	9.249
3	*** Haidian District, Beijing**	462.510	**69.659**	53	Hongshan District, Wuhan, Hubei	98.984	16.433
4	*** Xicheng District, Beijing**	392.431	**63.145**	54	Liwan District, Guangzhou, Guangdong	97.207	14.085
5	*** Binhai New District, Tianjin**	346.719	**46.273**	55	** Songjiang District, Shanghai	96.976	7.538
6	**Tianhe District, Guangzhou, Guangdong**	339.376	**56.338**	56	Wuzhong District, Suzhou, Jiangsu	94.562	5.958
7	**Jinshui District, Zhengzhou, Henan**	330.147	**48.129**	57	Shushan District, Hefei, Anhui	92.099	14.524
8	**Nanhai District, Foshan, Guangdong**	294.239	**36.169**	58	Shangcheng District, Hangzhou, Zhejiang	87.440	11.876
9	* Minhang District, Shanghai	264.734	25.472	59	Furong District, Changsha, Hunan	87.145	13.865
10	Shunde District, Foshan, Guangdong	261.456	35.519	60	* Yuhang District, Hangzhou, Zhejiang	86.637	8.118
11	* Kunshan City, Suzhou, Jiangsu	259.578	29.158	61	Xiacheng District, Hangzhou, Zhejiang	84.837	10.776
12	**Yuexiu District, Guangzhou, Guangdong**	241.868	**41.156**	62	Jiangbei District, Chongqing	84.509	13.103
13	**Dongcheng District, Beijing**	232.009	**38.057**	63	* Jianggan District, Hangzhou, Zhejiang	83.884	7.702
14	Jing'an District, Shanghai, China	220.741	30.315	64	Lixia District, Jinan, Shandong	83.346	13.077
15	* Yanta District, Xi'an, Shaanxi	209.401	31.498	65	Beilin District, Xi'an, Shaanxi	82.966	13.883
16	* Jiading District, Shanghai	204.036	19.892	66	Gulou District, Fuzhou, Fujian	81.949	13.050
17	Huangpu District, Guangzhou, Guangdong	195.110	28.540	67	Qiaokou District, Wuhan, Hubei	81.603	15.711
18	Guancheng Huizu District, Zhengzhou, Henan	193.564	27.165	68	* Huqiu District, Suzhou, Jiangsu	81.518	10.943
19	* Fengtai District, Beijing, China	190.931	23.532	69	Hanyang District, Wuhan, Hubei	80.123	13.243
20	Haizhu District, Guangzhou, Guangdong	189.168	29.564	70	Qixia District, Nanjing, Jiangsu	79.643	9.148
21	Baoshan District, Shanghai	177.678	15.940	71	* Yubei District, Chongqing	76.062	9.527
22	Baiyun District, Guangzhou, Guangdong	174.711	18.603	72	Hongkou District, Shanghai	75.882	10.748
23	Longgang District, Shenzhen, Guangdong	174.180	25.870	73	** Cixi City, Ningbo, Zhejiang	74.841	6.248
24	Chancheng District, Foshan, Guangdong	172.088	25.488	74	Chang'an District, Shijiazhuang, Hebei	72.902	5.405
25	Nanshan District, Shenzhen, Guangdong	172.045	33.033	75	Dongli District, Tianjin	71.831	5.262
26	Futian District, Shenzhen, Guangdong	168.581	31.446	76	Yuecheng District, Shaoxing, Zhejiang	71.339	3.348
27	* Huangpu District, Shanghai	165.727	26.004	77	Xinhua District, Shijiazhuang, Hebei	70.158	5.225

Table A4. *Cont.*

Index	County	Mean	Slope	Index	County	Mean	Slope
28	Panyu District, Guangzhou, Guangdong	164.036	19.444	78	* Gongshu District, Hangzhou, Zhejiang	69.477	6.462
29	* Yangpu District, Shanghai	162.899	23.062	79	* Xihu District, Hangzhou, Zhejiang	68.700	5.964
30	* Xuhui District, Shanghai	160.993	22.767	80	** Wujiang District, Suzhou, Jiangsu	68.296	6.781
31	Zhongyuan District, Zhengzhou, Henan	151.620	17.461	81	Nanan District, Chongqing	68.005	9.946
32	Wuchang District, Wuhan, Hubei	146.719	27.018	82	* Changshu City, Suzhou, Jiangsu	67.862	7.083
33	New Downtown, Urumqi, Xinjiang	141.533	19.474	83	Qinhuai District, Nanjing, Jiangsu	67.843	11.469
34	** Jiangyin City, Wuxi, Jiangsu	136.917	18.306	84	* Lianhu District, Xi'an, Shaanxi	67.737	10.376
35	Bao'an District, Shenzhen, Guangdong	136.839	18.738	85	** Yinzhou District, Ningbo, Zhejiang	67.608	6.450
36	* Weiyang District, Xi'an, Shaanxi	133.598	17.374	86	* Qingpu District, Shanghai	67.512	5.072
37	Jiangan District, Wuhan, Hubei	126.465	24.392	87	* Zhangjiagang City, Suzhou, Jiangsu	67.297	9.381
38	Jianghan District, Wuhan, Hubei	126.376	24.863	88	Huadu District, Guangzhou, Guangdong	66.779	6.616
39	** Xiaoshan District, Hangzhou, Zhejiang	123.029	8.703	89	Kaifu District, Changsha, Hunan	66.408	7.216
40	Putuo District, Shanghai, China	122.009	14.675	90	** Shunyi District, Beijing	65.801	6.710
41	* Binjiang District, Hangzhou, Zhejiang	119.847	15.289	91	Luohu District, Shenzhen, Guangdong	65.140	11.940
42	* Xinwu District, Wuxi, Jiangsu	117.225	15.207	92	* Xinbei District, Changzhou, Jiangsu	64.892	6.819
43	Changning District, Shanghai	116.156	14.799	93	Wangcheng District, Changsha, Hunan	64.199	7.006
44	* Liangxi District, Wuxi, Jiangsu	110.816	15.538	94	* Shijingshan District, Beijing	64.130	8.554
45	* Daxing District, Beijing, China	110.582	13.950	95	* Gusu District, Suzhou, Jiangsu	64.094	8.035
46	Gulou District, Nanjing, Jiangsu	109.536	17.910	96	* Cangshan District, Fuzhou, Fujian	63.415	7.207
47	Longhua District, Shenzhen, Guangdong	108.919	16.890	97	Jianxi District, Luoyang, Henan	62.566	6.272
48	Qiaoxi District, Shijiazhuang, Hebei	108.873	11.334	98	Erqi District, Zhengzhou, Henan	62.031	7.122
49	Yuhua District, Changsha, Hunan	108.205	14.109	99	* Shapingba District, Chongqing	60.458	7.867
50	** Wujin District, Changzhou, Jiangsu	105.131	11.475	100	Gulou District, Xuzhou, Jiangsu	59.920	8.413

Note: * means $p < 0.05$, ** means $p < 0.01$; the top 10 cities in terms of AGE increase are given in bold; unit of Mean, Slope is million CNY·ha, million CNY·ha/year, respectively.

References

1. Kumar, P.; Sharma, A. Assessing the monthly heat stress risk to society using thermal comfort indices in the hot semi-arid climate of India. *Mater. Today Proc.* **2022**, *61*, 132–137. [CrossRef]

2. Nandi, S.; Swain, S. Analysis of heatwave characteristics under climate change over three highly populated cities of South India: A CMIP6-based assessment. *Environ. Sci. Pollut. Res.* **2022**, *30*, 99013–99025. [CrossRef] [PubMed]
3. Russo, E.; Domeisen, D. A global comparison of heatwave magnitude indices using ERA5 reanalysis data (EMS2022-176). EMS2022. *Copernic. Meet.* **2022**, *19*, 176.
4. Ma, F.; Yuan, X. Impact of climate and population changes on the increasing exposure to summertime compound hot extremes. *Sci. Total Environ.* **2021**, *772*, 145004. [CrossRef]
5. Thompson, V.; Kennedy-Asser, A.T.; Vosper, E.; Lo, Y.T.E.; Huntingford, C.; Andrews, O.; Collins, M.; Hegerl, G.C.; Mitchell, D. The 2021 western North America heatwave among the most extreme events ever recorded globally. *Sci. Adv.* **2022**, *8*, eabm6860. [CrossRef] [PubMed]
6. Lin, H.; Mo, R.; Vitart, F. The 2021 Western North American Heatwave and Its Subseasonal Predictions. *Geophys. Res. Lett.* **2022**, *49*, e2021GL097036. [CrossRef]
7. Silberner, J. Heatwave causes hundreds of deaths and hospitalisations in Pacific north west. *Br. Med. J.* **2021**, *374*, n1696. [CrossRef] [PubMed]
8. Campbell, S.; Remenyi, T.A.; White, C.J.; Johnston, F.H. Heatwave and health impact research: A global review. *Health Place* **2018**, *53*, 210–218. [CrossRef]
9. Ullah, S.; You, Q.; Chen, D.; Sachindra, D.A.; AghaKouchak, A.; Kang, S.; Li, M.; Zhai, P.; Ullah, W. Future Population Exposure to Daytime and Nighttime Heatwaves in South Asia. *Earth's Future* **2022**, *10*, e2021EF002511. [CrossRef]
10. Perkins-Kirkpatrick, S.E.; Gibson, P.B. Changes in regional heatwave characteristics as a function of increasing global temperature. *Sci. Rep.* **2017**, *7*, 12256. [CrossRef] [PubMed]
11. Zhang, Y.; Mao, G.; Chen, C.; Lu, Z.; Luo, Z.; Zhou, W. Population exposure to concurrent daytime and nighttime heatwaves in Huai River Basin, China. *Sustain. Cities Soc.* **2020**, *61*, 102309. [CrossRef]
12. Yaglou, C.P.; Minaed, D. Control of Heat Casualties at Military Training Centers. *Arch. Indust. Health* **1957**, *16*, 302–316.
13. Huang, Z.; Chen, H.; Tian, H. Research on the Heatwave Index. *Meteorol. Mon.* **2011**, *37*, 345–351.
14. Wang, L.; Rohli, R.V.; Lin, Q.; Jin, S.; Yan, X. Impact of Extreme Heatwaves on Population Exposure in China Due to Additional Warming. *Sustainability* **2022**, *14*, 11458. [CrossRef]
15. Yin, C.; Yang, F.; Wang, J.; Ye, Y. Spatiotemporal distribution and risk assessment of heatwaves based on apparent temperature in the One Belt and One Road Region. *Remote Sens.* **2020**, *12*, 1174. [CrossRef]
16. Krummenauer, L.; Costa, L.; Prahl, B.F.; Kropp, J.P. Future heat adaptation and exposure among urban populations and why a prospering economy alone won't save us. *Sci. Rep.* **2021**, *11*, 1–14. [CrossRef]
17. Mora, C.; Dousset, B.; Caldwell, I.R.; Powell, F.E.; Geronimo, R.C.; Bielecki, C.R.; Counsell, C.W.; Dietrich, B.S.; Johnston, E.T.; Louis, L.V.; et al. Global risk of deadly heat. *Nat. Clim. Change* **2017**, *7*, 501–506. [CrossRef]
18. Nishant, N.; Ji, F.; Guo, Y.; Herold, N.; Green, D.; Virgilio, G.D.; Beyer, K.; Riley, M.L.; Perkins-Kirkpatrick, S. Future population exposure to Australian heatwaves. *Environ. Res. Lett.* **2022**, *17*, 064030. [CrossRef]
19. Ullah, I.; Saleem, F.; Iyakaremye, V.; Yin, J.; Ma, X.; Syed, S.; Hina, S.; Asfaw, T.G.; Omer, A. Projected Changes in Socioeconomic Exposure to Heatwaves in South Asia Under Changing Climate. *Earth's Future* **2022**, *10*, e2021EF002240. [CrossRef]
20. Raei, E.; Nikoo, M.R.; AghaKouchak, A.; Mazdiyasni, O.; Sadegh, M. GHWR, a multi-method global heatwave and warm-spell record and toolbox. *Sci. Data* **2018**, *5*, 180206. [CrossRef] [PubMed]
21. Moss, R.H.; Edmonds, J.A.; Hibbard, K.A.; Manning, M.R.; Rose, S.K.; van Vuuren, D.P.; Carter, T.R.; Emori, S.; Kainuma, M.; Kram, T.; et al. The next generation of scenarios for climate change research and assessment. *Nature* **2010**, *463*, 747–756. [CrossRef]
22. Wu, W.; Liu, Q.; Li, H.; Huang, C. Spatiotemporal Distribution of Heatwave Hazards in the Chinese Mainland for the Period 1990–2019. *Int. J. Environ. Res. Public Health* **2023**, *20*, 1532. [CrossRef] [PubMed]
23. Li, L.; Zha, Y. Population exposure to extreme heat in China: Frequency, intensity, duration and temporal trends. *Sustain. Cities Soc.* **2020**, *60*, 102282. [CrossRef]
24. Sun, S.; Dai, T.-L.; Wang, Z.-Y.; Chou, J.-M.; Chao, Q.-C.; Shi, P.-J. Projected increases in population exposure of daily climate extremes in eastern China by 2050. *Adv. Clim. Change Res.* **2021**, *12*, 804–813. [CrossRef]
25. Brandt, L.; Lim, K. Opening up in the 21st century: A quantitative accounting of Chinese export growth. *J. Int. Econ.* **2024**, *150*, 103895. [CrossRef]
26. Sang, M.; Jiang, J.; Huang, X.; Zhu, F.; Wang, Q. Spatial and temporal changes in population distribution and population projection at county level in China. *Humanit. Soc. Sci. Commun.* **2024**, *11*, 1–15. [CrossRef]
27. Duan, R.; Huang, G.; Li, Y.; Zheng, R.; Wang, G.; Xin, B.; Tian, C.; Ren, J. Ensemble Temperature and Precipitation Projection for Multi-Factorial Interactive Effects of GCMs and SSPs: Application to China. *Front. Environ. Sci.* **2021**, *9*, 742326. [CrossRef]
28. Ding, T.; Qian, W. Geographical patterns and temporal variations of regional dry and wet heatwave events in China during 1960–2008. *Adv. Atmos. Sci.* **2011**, *28*, 322–337. [CrossRef]
29. Liao, W.; Li, D.; Malyshev, S.; Shevliakova, E.; Zhang, H.; Liu, X. Amplified Increases of Compound Hot Extremes Over Urban Land in China. *Geophys. Res. Lett.* **2021**, *48*, e2020GL091252. [CrossRef]

30. Sun, Y.; Zhang, X.; Zwiers, F.W.; Song, L.; Wan, H.; Hu, T.; Yin, H.; Ren, G. Rapid increase in the risk of extreme summer heat in Eastern China. *Nat. Clim. Change* **2014**, *4*, 1082–1085. [CrossRef]
31. Wang, J.X.L.; Gaffen, D.J. Trends in Extremes of Surface Humidity, Temperature, and Summertime Heat Stress in China. *Adv. Atmos. Sci.* **2001**, *18*, 742–751. [CrossRef]
32. Bibi, S.; Wang, L.; Li, X.; Zhou, J.; Chen, D.; Yao, T. Climatic and associated cryospheric, biospheric, and hydrological changes on the Tibetan Plateau: A review. *Int. J. Climatol.* **2018**, *38*, e1–e17. [CrossRef]
33. Fan, Z.-X.; Bräuning, A.; Thomas, A.; Li, J.-B.; Cao, K.-F. Spatial and temporal temperature trends on the Yunnan Plateau (Southwest China) during 1961–2004. *Int. J. Climatol.* **2011**, *31*, 2078–2090. [CrossRef]
34. Wang, Q.; Zhai, P.-M.; Qin, D.-H. New perspectives on 'warming–wetting' trend in Xinjiang, China. *Adv. Clim. Change Res.* **2020**, *11*, 252–260. [CrossRef]
35. Zhang, J.; Yang, Z.; Wu, L.; Yang, K. Summer high temperature extremes over Northeastern China predicted by spring soil moisture. *Sci. Rep.* **2019**, *9*, 12577. [CrossRef] [PubMed]
36. Liu, X.; Tang, Q.; Zhang, X.; Sun, S. Projected Changes in Extreme High Temperature and Heat Stress in China. *J. Meteorol. Res.* **2018**, *32*, 351–366. [CrossRef]
37. Luo, M.; Lau, N.-C. Characteristics of summer heat stress in China during 1979–2014: Climatology and long-term trends. *Clim. Dyn.* **2019**, *53*, 5375–5388. [CrossRef]
38. Russo, S.; Sillmann, J.; Sippel, S.; Barcikowska, M.J.; Ghisetti, C.; Smid, M.; O'Neill, B. Half a degree and rapid socioeconomic development matter for heatwave risk. *Nat. Commun.* **2019**, *10*, 136. [CrossRef] [PubMed]
39. Yang, X.; Tian, Z.; Sun, L.; Chen, B.; Tubiello, F.N.; Xu, Y. The impacts of increased heat stress events on wheat yield under climate change in China. *Clim. Change* **2017**, *140*, 605–620. [CrossRef]
40. Feng, Y.; Sun, F.; Liu, W.; Chen, J.; Wang, H.; Guo, Q.; Wang, Y.; Zhang, Q.; Sang, Y.-F. Changes in compound hot and dry day and population exposure across China under climate change. *Int. J. Climatol.* **2022**, *42*, 2935–2949. [CrossRef]
41. Stevens, F.R.; Gaughan, A.E.; Nieves, J.J.; King, A.; Sorichetta, A.; Linard, C.; Tatem, A.J. Comparisons of two global built area land cover datasets in methods to disaggregate human population in eleven countries from the global South. *Int. J. Digit. Earth* **2020**, *13*, 78–100. [CrossRef]
42. Yi, L.; Xiong, L.; Yang, X. Method of Pixelizing GDP Data Based on the GIS. *J. Gansu Sci.* **2006**, *2*, 54–58.
43. The Rising Lab. *Index Model of Cities' Business Attractiveness in China*; The Rising Lab.: Southbank, VIC, Australia, 2021.
44. He, C.; Liu, Z.; Xu, M.; Lu, W. Dataset of urban built-up area in China (1992–2020) V1.0. In *A Big Earth Data Platform for Three Poles*; Dataset; A Big Earth Data Platform for Three Poles: Lanzhou, China, 2022.
45. Chen, Y.; Guo, F.; Wang, J.; Cai, W.; Wang, C.; Wang, K. Provincial and gridded population projection for China under shared socioeconomic pathways from 2010 to 2100. *Sci. Data* **2020**, *7*, 83. [CrossRef] [PubMed]
46. Peng, W.; Zhang, W.; Liu, J.; He, P.; Wang, J.; Huang, L.; Zhang, B. Analysis and intervention of heatwave related economic loss: Comprehensive insights from supply, demand, and public expenditure into the relationship between the influencing factors. *J. Environ. Manag.* **2023**, *326*, 116654.
47. Sun, X.; Ge, F.; Fan, Y.; Zhu, S.; Chen, Q. Will population exposure to heat extremes intensify over Southeast Asia in a warmer world? *Environ. Res. Lett.* **2022**, *17*, 044006. [CrossRef]
48. Xia, Y.; Li, Y.; Guan, D.; Tinoco, D.M.; Xia, J.; Yan, Z.; Yang, J.; Liu, Q.; Huo, H. Assessment of the economic impacts of heatwaves: A case study of Nanjing, China. *J. Clean. Prod.* **2018**, *171*, 811–819. [CrossRef]
49. Chen, H.; Sun, J. Increased population exposure to precipitation extremes in China under global warming scenarios. *Atmos. Ocean. Sci. Lett.* **2020**, *13*, 63–70. [CrossRef]
50. Luo, K.; Li, G.; Fang, C.; Sun, S. PM2.5 mitigation in China: Socioeconomic determinants of concentrations and differential control policies. *J. Environ. Manag.* **2018**, *213*, 47–55. [CrossRef] [PubMed]
51. Chen, J.; Liu, Y.; Pan, T.; Ciais, P.; Ma, T.; Liu, Y.; Yamazaki, D.; Ge, Q.; Peñuelas, J. Global socioeconomic exposure of heat extremes under climate change. *J. Clean. Prod.* **2020**, *277*, 123275. [CrossRef]
52. Yin, C.; Yang, Y.; Chen, X.; Yue, X.; Liu, Y.; Xin, Y. Changes in global heatwaves and its socioeconomic exposure in a warmer future. *Clim. Risk Manag.* **2022**, *38*, 100459. [CrossRef]
53. Xie, W.; Zhou, B.; Han, Z.; Xu, Y. Substantial increase in daytime-nighttime compound heatwaves and associated population exposure in China projected by the CMIP6 multimodel ensemble. *Environ. Res. Lett.* **2022**, *17*, 045007. [CrossRef]
54. You, H.; Yang, J.; Xue, B.; Xiao, X.; Xia, J.; Jin, C.; Li, X. Spatial evolution of population change in Northeast China during 1992–2018. *Sci. Total Environ.* **2021**, *776*, 146023. [CrossRef]
55. Yang, J.; Zhou, M.; Ren, Z.; Li, M.; Wang, B.; Liu, D.L.; Ou, C.-Q.; Yin, P.; Sun, J.; Tong, S.; et al. Projecting heat-related excess mortality under climate change scenarios in China. *Nat. Commun.* **2021**, *12*, 1039. [CrossRef] [PubMed]
56. Zhao, Y.; Sultan, B.; Vautard, R.; Braconnot, P.; Wang, H.J.; Ducharne, A. Potential escalation of heat-related working costs with climate and socioeconomic changes in China. *Proc. Natl. Acad. Sci. USA* **2016**, *113*, 4640–4645. [CrossRef] [PubMed]

57. Gao, J.; Liu, L.; Wu, S. Hazards of extreme events in China under different global warming targets. *Big Earth Data* **2020**, *4*, 153–174. [CrossRef]
58. Wu, D.; Hu, Z. Increasing compound drought and hot event over the Tibetan Plateau and its effects on soil water. *Ecol. Indic.* **2023**, *153*, 110413. [CrossRef]
59. You, Q.; Wu, F.; Shen, L.; Pepin, N.; Jiang, Z.; Kang, S. Tibetan Plateau amplification of climate extremes under global warming of 1.5 °C, 2 °C and 3 °C. *Glob. Planet. Change* **2020**, *192*, 103261. [CrossRef]
60. Gao, C.; Ge, H.; Lu, Y.; Wang, W.; Zhang, Y. Decoupling of provincial energy-related CO2 emissions from economic growth in China and its convergence from 1995 to 2017. *J. Clean. Prod.* **2021**, *297*, 126627. [CrossRef]
61. Wu, Y.; Tam, V.; Shuai, C.; Shen, L.; Zhang, Y.; Liao, S. Decoupling China's economic growth from carbon emissions: Empirical studies from 30 Chinese provinces (2001–2015). *Sci. Total Environ.* **2019**, *656*, 576–588. [CrossRef] [PubMed]
62. Naumann, G.; Cammalleri, C.; Mentaschi, L.; Feyen, L. Increased economic drought impacts in Europe with anthropogenic warming. *Nat. Clim. Change* **2021**, *11*, 485–491. [CrossRef]
63. Wang, A.; Tao, H.; Wu, Q.; Huang, J.; Zhang, B.; Wang, Y. Increasing urban and rural population exposures to warm-season concurrent hot days and nights on the North China Plain. *Int. J. Climatol.* **2022**, *42*, 7938–7950. [CrossRef]
64. Gasparrini, A.; Guo, Y.; Hashizume, M.; Lavigne, E.; Zanobetti, A.; Schwartz, J.; Tobias, A.; Tong, S.; Rocklöv, J.; Forsberg, B.; et al. Mortality risk attributable to high and low ambient temperature: A multicountry observational study. *The Lancet* **2015**, *386*, 369–375. [CrossRef] [PubMed]
65. Li, M.; Gu, S.; Bi, P.; Yang, J.; Liu, Q. Heatwaves and Morbidity: Current Knowledge and Further Direction-A Comprehensive Literature Review. *Int. J. Environ. Res. Public Health* **2015**, *12*, 5256–5283. [CrossRef] [PubMed]
66. Chambers, J. Global and cross-country analysis of exposure of vulnerable populations to heatwaves from 1980 to 2018. *Clim. Change* **2020**, *163*, 539–558. [CrossRef]
67. Fischer, E.M.; Schär, C. Consistent geographical patterns of changes in high-impact European heatwaves. *Nat. Geosci.* **2010**, *3*, 398–403. [CrossRef]
68. Lin, L.; Ge, E.; Liu, X.; Liao, W.; Luo, M. Urbanization effects on heatwaves in Fujian Province, Southeast China. *Atmos. Res.* **2018**, *210*, 123–132. [CrossRef]
69. Trigo, R.M.; García-Herrera, R.; Díaz, J.; Trigo, I.F.; Valente, M.A. How exceptional was the early August 2003 heatwave in France? *Geophys. Res. Lett.* **2005**, *32*, L10701. [CrossRef]
70. Wang, Y.; Zhao, N.; Wu, C.; Quan, J.; Chen, M. Future population exposure to heatwaves in 83 global megacities. *Sci. Total Environ.* **2023**, *888*, 164142. [CrossRef] [PubMed]
71. Wang, Y.; Zhao, N.; Yin, X.; Wu, C.; Chen, M.; Jiao, Y.; Yue, T. Global future population exposure to heatwaves. *Environ. Int.* **2023**, *178*, 108049. [CrossRef] [PubMed]
72. Yang, Y.; Zhao, N.; Wang, Y.; Chen, M. Variations in summertime compound heat extremes and their connections to urbanization in China during 1980–2020. *Environ. Res. Lett.* **2022**, *17*, 064024. [CrossRef]
73. Wang, A.; Tao, H.; Ding, G.; Zhang, B.; Huang, J.; Wu, Q. Global cropland exposure to extreme compound drought heatwave events under future climate change. *Weather. Clim. Extrem.* **2023**, *40*, 100559. [CrossRef]
74. Wang, J.; Chen, Y.; Tett, S.F.B.; Stone, D.; Nie, J.; Feng, J.; Yan, Z.; Zhai, P.; Ge, Q. Storyline attribution of human influence on a record-breaking spatially compounding flood-heat event. *Sci. Adv.* **2023**, *9*, eadi2714. [CrossRef] [PubMed]

Disclaimer/Publisher's Note: The statements, opinions and data contained in all publications are solely those of the individual author(s) and contributor(s) and not of MDPI and/or the editor(s). MDPI and/or the editor(s) disclaim responsibility for any injury to people or property resulting from any ideas, methods, instructions or products referred to in the content.